

University of Alberta

**CHARACTERIZATION AND CALCULATION OF
FRACTURE TOUGHNESS FOR HIGH GRADE PIPES**

by

Cheng Cen

A thesis submitted to the Faculty of Graduate Studies and Research
in partial fulfillment of the requirements for the degree of

Master of Science

Department of Mechanical Engineering

© Cheng Cen

Spring 2013

Edmonton, Alberta

Permission is hereby granted to the University of Alberta Libraries to reproduce single copies of this thesis and to lend or sell such copies for private, scholarly, or scientific research purposes only. Where the thesis is converted to, or otherwise made available in digital form, the University of Alberta will advise potential users of the thesis of these terms.

The author reserves all other publication and other rights in association with the copyright in the thesis and, except as herein before provided, neither the thesis nor any substantial portion thereof may be printed or otherwise reproduced in any material form whatsoever without the author's prior written permission.

Abstract

The classical Battelle two-curve method is proved to be non-conservative in calculating the arrest fracture toughness of high grade line pipes. In this thesis, first, the concept of “limit (crack) speed” is introduced to the existing two-curve method, which leads to a modified two-curve method (LS-TCM) that could give more accurate calculation of fracture toughness in some cases for both low and high grade pipes. Several other new ideas and approaches are also proposed to calculate fracture toughness of all grade pipes, and their applicability for high grade pipes is discussed with comparison to available known data. Some comments are given about how to choose an appropriate formula to calculate fracture toughness for high grade pipes. Finally, the relationship between the three basic parameters for characterizing fracture toughness, CVN, DWTT and CTOA, is also discussed, in order to give designers helpful advice about how to choose the parameters to characterize fracture toughness of line pipes.

Acknowledgements

I would like to take this opportunity to express my gratitude to those who have assisted me in writing this thesis and help me during my study in Edmonton. My primary thanks go to Professor Chongqing Ru, who offered me the opportunity to pursue my Master degree at University of Alberta. I also would like to thank Mr. Jian Wu and Mr. Mingzhao Jin for their helpful discussions during my thesis writing.

Abstract

Acknowledgements

Table of Contents

List of Figures

List of Tables

List of Abbreviations

Table of Contents

Chapter 1 Introduction..... 1

 1.1 Introduction to high strength steel line pipes in industries..... 1

 1.1.1 Lower grades 3

 1.1.2 Higher grades 4

 1.2 Introduction to fracture toughness..... 5

 1.3 Introduction to Charpy V-Notch (CVN) energy 7

 1.3.1 CVN test 7

 1.3.2 CVN energy in Battelle two-curve method (Battelle-TCM) and Maxey single-curve method (Maxey-SCM)..... 8

 1.3.3 Corrections of CVN energy in the Battelle-TCM..... 9

 1.4 Introduction to Drop-weight Tear Test (DWTT) energy 13

 1.4.1 DWTT specimens 13

 1.4.2 Correlation between DWTT and CVN energies..... 15

 1.5 Introduction to Crack Tip Open Angle (CTOA)..... 15

 1.6 Objectives of this thesis 18

Chapter 2 Analysis of Charpy V-Notch (CVN) energy..... 20

 2.1 A “Limit Speed” based Two-curve Method (LS-TCM)..... 20

 2.1.1 Database for TCM calculation..... 20

2.1.2 Derivation of “Limit Speed” based Two-curve Method (LS-TCM).....	23
2.1.3 Calculation of fracture toughness using LS-TCM.....	25
2.1.4 Calculation of crack speed using LS-TCM.....	30
2.1.5 Modification to the Folias Factor.....	32
2.1.6 Remarks.....	34
2.2 Single-curve method (SCM).....	35
2.2.1 Discussion about different single-curve methods.....	35
2.2.2 Modifications to single-curve method developed by Vogt (Vogt-SCM).....	37
2.2.3 Comparison between Battelle-TCM and Maxey-SCM.....	39
2.2.4 Remarks.....	42
Chapter 3 Analysis of Drop-weight Tear Test (DWTT) energy.....	44
3.1 Derivation of DWTT Single-curve Method (DWTT-SCM).....	44
3.2 Discussion about the linear relation between DWTT and CVN energy.....	48
3.3 Derivation of TCM expressed with DWTT energy (DWTT-TCM).....	55
3.4 Remarks.....	55
Chapter 4 Analysis of Crack Tip Open Angle (CTOA).....	57
4.1 Introduction of CTOA Single-curve Method (CTOA-SCM).....	57
4.2 Derivation of Linear relation between CTOA and CVN.....	59
4.3 Derivation of TCM expressed with CTOA (CTOA-TCM).....	63
4.4 Comparison between CTOA-SCM, Battelle-TCM, LS-TCM, Maxey-SCM and Vogt-SCM:.....	64
4.5 Remarks.....	66
Chapter 5 Summary and Future Work.....	68
Bibliography.....	71

List of Figures

Figure 1.1 Example of crack propagate along pipes with increasing toughness.....	7
Figure 2-1 Sample comparison of two-curves for Battelle-TCM and LS-TCM.....	27
Figure 2-2 Fracture toughness calculated from three two-curve methods.....	29
Figure 2-3 Comparison of calculated crack speed and test speed.....	32
Figure 2-4 fracture toughness calculated using different Folias factors	33
Figure 2-5 fracture toughness calculated by different single-curve methods.....	37
Figure 2-6 Result for modification method I for Vogt-SCM.....	38
Figure 2-7 Result for modification method II for Vogt-SCM.	39
Figure 2-8 Vogt-SCM and LS-TCM both improves the fracture toughness calculation of original Battelle-TCM and Maxey-SCM	42
Figure 3-1 Curve fitting of result of DWTT-SCM to experiment data.....	46
Figure 3-2 Curve fitting of the results in Table 3-3 to the equation from reference [37].	47
Figure 3-3 The linear ratio of DWTT/CVN for X60.....	49
Figure 3-4 The linear ratio of DWTT/CVN for X65.....	49
Figure 3-5 The linear ratio of DWTT/CVN for X70.....	50
Figure 3-6 The linear ratio of DWTT/CVN for X80.....	50
Figure 3-7 The linear ratio of DWTT/CVN for X100.....	51
Figure 3-8 The non-linear ratio of DWTT/CVN for X60.....	51
Figure 3-9 The non-linear ratio of DWTT/CVN for X65.....	52
Figure 3-10 The non-linear ratio of DWTT/CVN for X70.....	52
Figure 3-11 The non-linear ratio of DWTT/CVN for X80.....	53
Figure 3-12 The non-linear ratio of DWTT/CVN for X100.....	53
Figure 4-1 Curve fitting of predicted CTOA from eqn.(4.2) and real CTOA value.....	59
Figure 4-2 The linearity between CTOA-SCM and CVN energy values from experiment. ...	60
Figure 4-3 The relationship between crack speed and CTOA-SCM.....	62
Figure 4-4 The relationship between crack speed and CTOA, from reference [39].....	62
Figure 4-5 Comparison of fracture toughness calculated from different formulas.....	65

List of Tables

Table 1-1 typical material composition for different grade of pipes	5
Table 2-1 fracture toughness calculated by different two-curve methods.....	27
Table 2-2 crack speed calculation	3029
Table 2-3 fracture toughness calculated using different Folias factors.....	33
Table 2-4 fracture toughness calculated by different single-curve methods	35
Table 2-5 fracture toughness calculated by different methods	40
Table 3-1 range of CVN, CTOA and DWTT energy at different pipe grades	43
Table 3-2 data for deriving SCM for DWTT energy	44
Table 3-3 comparison of predicted DWTT-SCM results and predicted Vogt-SCM results ...	46
Table 4-1 data for deriving the constants in eqn. 4.1.....	57
Table 4-2 data for deriving the constants in eqn. 4.3.....	60
Table 4-3 comparison between crack speeds and single-curve method CTOA values.	62
Table 4-4 comparison of the fracture toughness calculated from different formulas	63

List of Abbreviations

CVN:	Charpy V-notch
TCM:	Two-curve method
SCM:	Single-curve method
Battelle-TCM:	Battelle two-curve method
Maxey-SCM:	Maxey single-curve method
CSM-TCM:	CSM Adjustment to the Battelle-TCM
Leis-TCM:	Leis Adjustment to the Battelle-TCM
Wilkowski-TCM:	Wilkowski Adjustment to the Battelle-TCM
Higuchi-TCM:	Higuchi Adjustment to the Battelle-TCM
LS-TCM:	“Limit Speed” based two-curve method
Maxey-SCM:	Single-curve method developed by Maxey
AISI-SCM:	Single-curve method developed by AISI
Feanehough-SCM:	Single-curve method developed by Feanehough
Vogt-SCM:	Single-curve method developed by Vogt
DWTT:	Drop-weight tear test
EN-DWTT:	Embrittled-notch DWTT
PN-DWTT:	Pressed-notch DWTT
DWTT-SCM:	DWTT Single-curve method
DWTT-TCM:	DWTT Two-curve method
CTOA:	Crack tip open angle
CTOA-SCM:	CTOA Single-curve method
CTOA-TCM:	CTOA Two-curve method
CV-CTOA:	Charpy V-notch energy formula expressed by CTOA

Chapter 1

Introduction

1.1 Introduction to line pipes in industries

As the worldwide demand for natural gas has continued to grow since 1950s' [1], how to transport gas from sources which are increasingly remote from the centers of population has become the major challenge for gas companies. Among the options is the construction of long-distance high-capacity line pipes, particularly across the remote areas in Arctic North America, South America and Africa.

Based on an economic aspect, ExxonMobil [2] identified transportation cost as a key factor in the commercialization of remote gas resources in the early 1990's. The way to reduce the installation cost of a long-distance line pipe is to utilize higher strength steels; such an approach offers the possibility of reducing the ratio of pipe wall thickness to diameter, hence reducing the cost of materials and construction for a required throughput. Studies related to conceptual line pipes in North Africa, Eastern Europe and Arctic North America have identified 5 to 15 percent potential reductions in installed cost, resulted from the adoption of the high strength steel based designs and materials.

In response to the challenge of high strength steel requirements, pipe manufacturers and designers have collaborated to introduce a progressive evolution of higher grade pipes to the industry during the last 50 years [3]. The developments and changes in production techniques include the use of various forms of thermo-mechanical processing such as controlled rolling and

accelerated cooling. Most of the existing infrastructures have been used in pipes with pipe grade larger than X70, many thousands of kilometers of such pipes are transporting gas across all the inhabited continents.

The development of high-strength steels started more than 30 years ago [3], along with the introduction of thermo-mechanical rolling practices, and will continue in the future. In the early 1970s', the hot rolling and normalizing process route was replaced by thermo-mechanical rolling. The latter process enables materials up to grade X70 to be produced from steels that are micro-alloyed with Niobium and Vanadium and have a reduced carbon content. After a 20 years development this is now a fully satisfactory material technology for constructing line pipes with diameters up to 1200 mm, and operation pressures up to 100 bar. It shows a trend that, conceptual designs will focus on higher pressure and higher strength materials for the next generation of long distance high-capacity line pipes.

An improved processing method, consisting of thermo-mechanical rolling plus subsequent accelerated cooling, emerged in the 1980s'. By this method, it has become possible to produce higher strength line pipe infrastructures like X80 in Western Europe and North America, X80 having a further reduced carbon content and thereby excellent field weld ability.

Additions of Molybdenum, Copper and Nickel enable the strength level to be raised to that of grade X100 and X120, when the steel is still processed to plate by thermo-mechanical rolling plus modified accelerated cooling.

Line pipes are classified into different grades because of their different yield strength, the larger yield strength it possesses, the higher grade it belongs to.

1.1.1 Lower grades

1.1.1.1 X60

Starting from normalized X60 grade which was mainly used in the early 1970s', the combination of different types of microstructures contribute to increase mechanical strength and toughness of steels [4]. The steel typically contains 0.2% Carbon, 1.55% Manganese, 0.12% Vanadium, 0.03 % Niobium and 0.02% Nitrogen.

1.1.1.2 X70

In the early 1970s', grade StE 480.7 TM (X70) was introduced for the first time in a gas transmission line pipe construction project in Germany. Since then, grade X70 material has proven a very reliable material in the implementation of numerous line pipe projects. Reduction of pearlite content, grain refining, dislocation hardening and precipitation hardening all contributed to the development of X70 steel, with improved weld ability and favorable ductile-brittle transition temperatures.

1.1.1.3 X80

Following satisfactory experience gained with X70 line pipe, longitudinal welded X80 pipes were used in several line pipe projects in Europe and North America since 1984.

In 1984, grade X80 line pipe produced by EUROPIPE was used for the first time in the Megal II line pipe. Manganese-Niobium-Titanium steel, additionally alloyed with Copper and Nickel, was used for the production of the 13.6mm wall pipe.

Then grade X80 was used in a 3.2 km line pipe trial project in 1985 [5]. Subsequently, the material was used in the construction of several additional trial sections, as referred in Table 1-1.

1.1.2 Higher grades

1.1.2.1 X100 and X120

The development of grade X100 and X120 line pipes for high-pressure gas pipelines has been the common interest of steel manufacturers and major oil companies in the last 20 years [6]. The worldwide leader in developing grade X100 line pipes is EUROPIPE. Since 1995, EUROPIPE has developed different approaches to produce high strength materials.

The properties of pipes produced are carefully investigated for safe operation under high pressure in order to cope with the market requirements for enhanced pipe strength. The medium Carbon content of about 0.06% ensures excellent toughness as well as fully satisfactory field weld ability. Lean chemistry is selected from because of its high weld ability and low alloy cost. Traditionally quench and tempered process was employed to get high strength for the X100 or X120 grade pipes.

The prototype of X100 and X120 line pipes were produced in Sumitomo Metal's Kashima Steel Works. Slabs for plate were made by the continuous caster. The steel for X100 is 0.07%C-1.83%Mn-(Cu-Ni-Cr-Mo-Nb-Ti) and the steel for X120 is 0.05%C-1.56%Mn-(Cu-Ni-Cr-Mo-Nb-V-Ti-B). Material compositions for different grade of pipes can be referred in Table 1.1. The pipe sizes are 914 mm OD (Outer diameter) * 19 mm thick for X100, and 914 mm OD * 16 mm thick for X120.

Table 1-1 typical material composition for different grade of pipes, Ref [4-6]:

	Material composition
X60	0.2%C, 1.55%Mn, 0.12%V, 0.03%Ni, 0.02%N
X70	0.05%C, 1.7%Mn, 0.27%Mo, 0.075%Nb
X80	0.09%C, 1.9%Mn, 0.04%Ni, 0.02%Ti
X100	0.07%C, 1.83%Mn, 0.3%Mo, 0.24%Ni, 0.05%Nb, 0.024%Cu, 0.023%Cr, 0.019%Ti
X120	0.05%C, 1.56%Mn, 1.1%B, 0.27%Mo, 0.22%Ni, 0.21%Cr, 0.04%Nb, 0.029%Cu, 0.022%V, 0.017%Ti

1.1.2.2 Advantages for choosing high grade pipes

Take X120 and X70 as the example [2], X120 is economic than X70 from four aspects: the manipulating of X120 help reduces the material cost; the manipulating of X120 help to low the construction cost; X120 can be used to reduce the compression cost; X120 can be used to integrate the project savings.

1.2 Introduction to fracture toughness

The fracture propagation toughness of steel refers to the resistance of the material to rapid crack propagation [7]. The fracture propagation toughness can be taken as the energy required to create new fracture surfaces or to fracture a test specimen. The velocity of a propagating fracture is a function of fracture propagation toughness, pipe geometry, gas composition, operating temperature, and operating pressure.

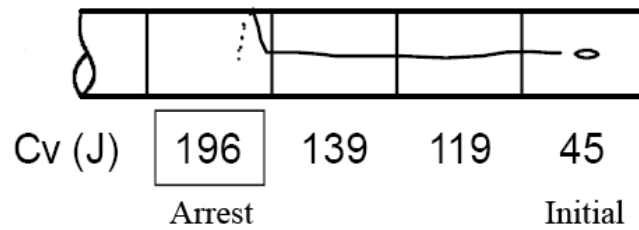
The driving force of a fracture is a function of the pressure at the tip of the moving fracture and the geometry of the pipe. The pressure at the fracture tip

is a function of the gas composition, its initial pressure and temperature, and the velocity of the fracture. In ductile fractures, when the fracture velocity is less than the velocity of sound in the gas at its initial temperature and pressure, the pressure at the tip of the crack will decay to a value less than the initial line pressure. For arrest to occur, the pressure required to create the fracture, which depends on the fracture propagation toughness, must exceed the pressure available to drive it.

The full-scale pipe fracture appearance and transition temperature are related to the fracture appearance and transition temperature of Charpy V-notch (CVN) and Drop-Weight Tear Test (DWTT) specimens. The full-scale propagation toughness has been correlated with CVN and DWTT upper-shelf or plateau energies and the expected percent shear appearance of the propagating fracture. Actually, the fracture toughness can be CVN plateau energy, DWTT energy, crack tip open angle (CTOA) or any other measurable properties that have correlations with fracture arrest.

The pipeline used in arrest toughness test or experiments are composed of pipe sectors connected with increasing toughness (in either CVN energy or DWTT energy form), see figure 1.1. An explosive is embedded in the initial pipe with lowest toughness, when explosion happens the gas inside the pipe decompresses and crack propagates. When crack propagates to the next sector, the toughness becomes higher therefore the resistance to crack propagation becomes higher. The crack propagation will finally stop in a sector of the pipe, and the toughness of that pipe (determined from CVN or DWTT test) is taken as the arrest toughness for given material, initial pressure and backfill conditions. The arrest toughness determined above will be used in industry as guidelines for piping constructions and maintenances.

Figure 1.1 example of crack propagate along pipes with increasing toughness.



1.3 Introduction to Charpy V-Notch (CVN) energy

1.3.1 CVN test

A CVN specimen is a small notched bar that is machined from the pipe, usually in the transverse direction [7]. The specimen is broken by an impact load from a pendulum on the side opposite to the notch while the specimen is supported at each end of the notched side. Charpy V-notch test specimen is a small size specimen that does not reflect the real thickness of the pipe. CVN energy equals to the potential energy of the overhead pendulum. A full thickness specimen has a thickness of 0.394 inches (10 mm), and the usually used two-thirds thickness Charpy V-Notch impact specimen has a thickness of 0.264 inches (6.7mm) with all other dimensions the same.

The Charpy V-notch energy determined from the test is then recorded as the toughness data for given materials. This material is used in test pipe production.

1.3.2 CVN energy in Battelle two-curve method (Battelle-TCM) and Maxey single-curve method (Maxey-SCM)

1.3.2.1 CVN in Battelle-TCM

The most frequently used analysis for ductile fracture toughness is the Battelle Two-Curve Method (Battelle-TCM) developed by Maxey [8-12]. In this method the minimum CVN upper-shelf energy was used in the calibration of a semi-empirical model for arrest. That work was conducted in the late 1960's involving X52 to X65 grade pipes with relatively low Charpy upper-shelf energies. This analysis procedure incorporates the gas decompression curve to account for two-phase decompression behavior of rich gases.

The CVN energy predicted from two-curve methods is used to forecasting the arrest toughness of line pipes in fracture arrest experiments. In fracture arrest experiments, the CVN energy predicted give designers ideas about in which pipe sector may the arrest happen.

Battelle-TCM is composed of three equations as follows:

$$\left\{ \begin{array}{l} V_f = 2.76 \times \frac{\sigma_{flow}}{\sqrt{C_v}} \times \left(\frac{P_d}{P_a} - 1 \right)^{\frac{1}{6}} \\ \frac{P_d}{P_i} = \left[\frac{V_d}{6V_a} + \frac{5}{6} \right]^7 \\ P_a = \frac{4}{3.33\pi} \cdot \frac{t}{D} \cdot \sigma_{flow} \cdot \cos^{-1} \exp \left(\frac{-18.75 \cdot \pi E \cdot C_v}{24 \sqrt{Dt} / 2 \cdot \sigma_{flow}^2} \right) \end{array} \right. \quad (1.1)$$

V_f : crack speed, m/s. V_d : decompression gas speed, m/s. V_a : acoustic speed, m/s. C_v : Charpy V-notch upper-shelf energy for a 2/3-thickness specimen, J.

P_d : decompressed pressure, MPa. P_a : arrest pressure, MPa. P_i : initial pressure, MPa. σ_{flow} : flow stress, MPa. D: outside diameter of the pipe, mm. t: pipe wall thickness, mm.

For minimum arrest condition, we have the following two additional equations, therefore totally five equations can solve the five unknowns ($C_v, V_f, V_d, P_d,$

P_a):

$$\begin{cases} V_f = V_d \\ \frac{dV_f}{dP_d} = \frac{dV_d}{dP_d} \end{cases} \quad (1.2)$$

1.3.2.2 CVN in Maxey-SCM

The Maxey-SCM is a closed-form equation derived from simulations conducted using the iterative SCM for a variety of design conditions [8]. The simple Maxey-SCM equation calculates an upper shelf Charpy energy value required to arrest a propagating ductile fracture. Due to its simplicity, the Maxey-SCM equation is cited extensively in a variety of codes and standards for pipeline design.

The general form of Maxey-SCM is written as:

$$C_{v-Maxey-SCM} = 0.709 \times 10^{-5} P_i^2 D^{2.333} t^{-1.667} \quad (1.3)$$

where $C_{v-Maxey-SCM}$ is the predicted minimum CVN energy required for arrest (in Joules), P_i is the initial pressure in the pipe (in MPa), D is the pipe diameter and t is the pipe wall thickness.

1.3.3 Corrections of CVN energy in the Battelle-TCM

The Battelle-TCM is still used frequently today. Nevertheless, as higher-grade steels have been developed, it is found from full-scale tests that a multiplier was needed on the minimum Charpy arrest energy calculated from the Battelle-TCM. Several researchers [13] have also suggested that a correction factor was needed on the Charpy energy as the Charpy energy value increased

above a certain level. This was a nonlinear correction factor larger than 1, since the Charpy energy predicted from Battelle-TCM is less than the tested Charpy energy when Charpy energy value surpassed a certain level.

1.3.3.1 CSM adjustment of the Battelle-TCM (CSM-TCM)

To address the discrepancies noted between the actual fracture toughness from full-scale tests and those values predicted by the Battelle-TCM model, Mannucci et al. [14] proposed the following correction factor:

$$CVN_{TCM-CSM} = 1.7 CVN_{Battelle-TCM} \quad (1.4)$$

where, $CVN_{TCM-CSM}$ is the adjusted Charpy V-notch toughness required for arrest, and $CVN_{Battelle-TCM}$ is the Charpy V-notch toughness predicted using the original Battelle Two-curve method.

This empirical factor was derived by directly comparing the Battelle-TCM model results to actual arrest toughness values from a number of full-scale fracture propagation tests on grade X100 steel pipe. The factor is intended to adjust the predicted curve to correlate with actual arrest toughness values. Based on recent burst test results, however, CSM recognized that this correction factor may be unsuitable and suggested that no new correction factor could be obtained.

1.3.3.2 Leis adjustment of the Battelle-TCM (Leis-TCM)

Leis et al. [15] proposed a correction factor for the Battelle-TCM that separates the contributions of the initiation and propagation portion of the Charpy energy. The original Battelle-TCM model was derived based on correlations with older pipeline steels for which absorbed energy values were dominated by dynamic (propagation) fracture. For newer steels with

apparently increased toughness, however, the energy required for initiation (i.e. contributions from plastic deformation and specimen geometry effects) becomes more significant. The proposed correction factor minimizes the contribution of the initiation energy, which does not necessarily represent the true dynamic fracture resistance of the material.

The resulting correction is given as follows:

$$CVN_{TCM-Leis} = CVN_{Battelle-TCM} + 0.002CVN_{Battelle-TCM}^{2.04} - 21.18 \quad (1.5)$$

where $CVN_{TCM-Leis}$ is the corrected prediction of Charpy V-notch toughness required for fracture arrest (in Joules).

The effect of this equation is to progressively increase the required CVN toughness values for increasing values of toughness as calculated using the Battelle-TCM. As such, it is only valid for pipes having a measured CVN toughness above 94 J. Below this value, it is recommended to use the original Battelle-TCM toughness value. Leis has demonstrated an improved correlation between the toughness values predicted from his formula and the actual fracture toughness from full-scale tests, as compared to the toughness values calculated from original Battelle-TCM.

1.3.3.3 Wilkowski adjustment of the Battelle-TCM (Wilkowski-TCM)

Similar to the method used by Leis, an adjustment to the Battelle-TCM was reported by Papka et al. [16], this adjustment is based on experiments and analysis performed by Wilkowski et al. [17]. In Wilkowski's experiments, the contributions of the initiation and propagation energy were separated by correlating test results from conventional CVN specimens and modified DWTT specimens (which minimized the initiation effects).

Based on this correlation, an adjustment to the original Battelle-TCM was developed that takes the following form:

$$CVN_{TCM-Wilkowski} = 0.056(0.1018CVN_{Battelle-TCM} + 10.29)^{2.597} - 16.8 \quad (1.6)$$

where, $CVN_{TCM-Wilkowski}$ is the corrected prediction of Charpy V-notch toughness required for fracture arrest (in Joules). This equation is similar to the Leis correction formula, in that the modified toughness is an increasing function of the calculated Battelle-TCM toughness value as Charpy energy increases.

1.3.3.4 Higuchi adjustment of the Battelle-TCM (Higuchi-TCM)

An important two-curve method developed by Ryota Higuchi et. al. (Higuchi-TCM) [18] is also included here. Different from other modifications to Battelle-TCM, this method focus on the modification of the fracture/crack speed, since the predicted crack speed from Battelle-TCM is less than real crack speed values for high grade pipes. The author adjusts the constants in Battelle-TCM to increase and therefore better correlate the predicted crack speed to the real crack speed.

However, the characterizing of fracture toughness by Higuchi-TCM is not discussed in the paper, we put the Higuchi-TCM here and compares it with Battelle-TCM and the “Limit Speed” based two-curve method (LS-TCM) we derived in section 2.1.2.

$$\left\{ \begin{array}{l} V_f = \alpha \cdot \frac{\sigma_{flow}}{\sqrt{C_v}} \cdot \left(\frac{P_d}{P_a} - 1 \right)^\beta \\ \frac{P_d}{P_i} = \left[\frac{V_d}{6V_a} + \frac{5}{6} \right]^7 \\ P_a = \lambda \cdot 0.380 \cdot \frac{t}{D} \cdot \sigma_{flow} \cdot \cos^{-1} \exp \left(\frac{-4.57 \cdot 10^7 \cdot C_v}{\sqrt{Dt/2} \cdot \sigma_{flow}^2} \right) \end{array} \right. \quad (1.7)$$

where $\alpha=0.670 \cdot [(Dt)/(D_0t_0)]^{1/4}$,

$\beta=0.393 \cdot (D/D_0)^{5/2} \cdot (t/t_0)^{-1/2}$,

$$\gamma = \frac{3.42}{\left[3.22 + 0.20 \cdot \left(\frac{t/D}{t_0/D_0} \right)^3 \right]}$$

$D_0=1219.2(\text{mm})$,

$t_0=18.3(\text{mm})$,

1.4 Introduction to Drop-weight Tear Test (DWTT) energy

Frequently the rising shelf, controlled-rolled steels exhibit separations for which the rising shelf Charpy energies do not fit to. The search for an alternate toughness measurement for the controlled-rolled steels led to an investigation of the drop-weight tear test (DWTT) energy as a measure of the fracture propagation toughness [19].

Over the last few decades, it has become recognized that the DWTT better represents the ductile fracture resistance of rising shelf controlled rolled steels than the Charpy test since it utilizes a specimen that has the full thickness of the pipe and has a fracture path long enough to reach steady-state fracture resistance. DWTT energy is taken as the potential energy of the hammer as it falls down to fracture the DWTT specimen.

1.4.1 DWTT specimens

1.4.1.1 Embrittled notch DWTT specimen and pressed notch DWTT specimen

Two kinds of DWTT energies are frequently used, the standard pressed notch

DWTT (PN-DWTT) energy and the embrittled notch DWTT (EN-DWTT) energy [20].

The PN-DWTT specimens exhibited constant upper shelf and has been adopted by API standard to define the ductile to brittle transition temperature of gas pipelines. The statical PN-DWTT is the preferred test method as compares to EN-DWTT since it is more economical and reproducible.

Wilkowski and many other investigators [19], [21] tried different ways of embrittling the notch of the DWTT specimen by depositing a brittle weld bead at the notch location in order to get a better measure of the fracture propagation energy and transition temperature. In this specimen, the width and length were changed but the base-metal fracture area remained constant at 2.8 inches, i.e., the same as in the standard PN-DWTT specimen. The EN-DWTT specimens is either statically pre-cracked (i.e., monotonically loaded to just beyond maximum load prior to impacting the specimen.) or deposited with brittle weld metal at the notch. Embrittled notch specimen could properly predict the full-scale brittle-to-ductile fracture behavior. It also showed that the total upper-shelf fracture energy in the EN-DWTT could be significantly lower than that in the PN-DWTT.

A linear relationship was obtained between the EN-DWTT energy and the standard PN-DWTT energy:

$$(E/A)_{EN-DWTT} = 175[(E/A)_{PN-DWTT}]^{0.385} - 1500 \quad (1.8)$$

Where $(E/A)_{EN-DWTT}$ is the total impact energy (E) of an embrittled notch DWTT specimen divided by the cross-sectional fracture surface area (A) of the specimen. $(E/A)_{PN-DWTT}$ is the total impact energy (E) of a pressed-notch DWTT specimen divided by the cross-sectional fracture surface area (A) of the specimen. The energy and the constant 1500 are in ft-lb/in².

1.4.2 Correlation between DWTT and CVN energies

There is no formulas for DWTT energy, however, the correlation between DWTT and CVN energies was put forward a long time ago [19].

In the mid-1970's, the toughness of line pipe steels increased significantly. Because of the high toughness of these steels, the energy capacity of the DWTT machine needs to be increased. This was actually the initial reason for determining a relationship between Charpy energy and pressed-notch DWTT energy. This relationship was first developed by Wilkowski for conventionally rolled steels and quenched and-tempered steels. The relationship is given in the following form:

$$DWTT = 3 * CVN + 300, ft - lb / in2 \quad (1.9)$$

At the same time Wilkowski modified the notch of a standard DWTT specimen in an attempt to exclude the initiation portion of the total specimen energy. It was envisioned that this would not only accurately capture the transition temperature, but also provide a better estimation of the true propagation resistance.

1.5 Introduction to Crack Tip Open Angle (CTOA)

1.5.1 CTOA as a measure of fracture toughness

With the introduction of modern low carbon and ultra high toughness steels, conventional measures of ductile fracture toughness (standard Charpy and DWTT energy) are under review, and alternatives are being studied [22]. As material strength, pipe diameter and operating pressure increased, requiring

greater fracture propagation resistance, the limitations of the Charpy energy approach became increasingly apparent [7]. This is because for modern steels, the Charpy test involves significant energy absorption contributions from processes not related to fracture propagation.

The crack tip opening angle (CTOA) [23], a formal fracture mechanics based parameter, was investigated to evaluate its appropriateness as a measure of high grade pipe ductile fracture toughness. There are different ways to define the CTOA, a typical definition for CTOA is the open angle 0.04 inches away from the crack tip.

CTOA is observed as the most convenient parameter during the inelastic dynamic fracture propagation of the line pipe steel [23]. It has been claimed that CTOA is a constant during steady state crack propagation [24] and therefore has the promise of being directly applied to full-scale pipeline fracture. Results of fracture mechanics tests at quasi-static rate were analyzed to examine the constancy of CTOA with crack growth in four modern low C, low S chemistries and thermo-mechanically controlled processed (TMCP) steels. The linear relation observed between load line displacements supports the concept of a constant CTOA during “steady state” crack propagation.

The CTOA may be a viable alternative to the Charpy energy for characterizing fracture, and therefore has particular promise for modern high strength line pipe where the significance of the Charpy energy is increasingly coming under question.

1.5.2 CTOA calculation

It will be necessary to ensure that the applied CTOA, which depends on

geometry and loading, is less than the critical material toughness value, labeled as $(CTOA)_c$.

By quantifying the maximum steady-state crack driving force $(CTOA)_{\max}$, that would occur with a given pipe geometry and initial gas pressure, it is then possible to specify the resistance required to preclude the steady state. The fracture event is then precluded, provided that:

$$(CTOA)_c > (CTOA)_{\max} \quad (1.10)$$

Where $(CTOA)_{\max}$ is the maximum steady-state value of the CTOA values calculated over the range of plausible crack speeds.

The routine to determine the maximum material toughness term, $(CTOA)_{\max}$, in inequality above is highly desirable. The three primary technical research elements combined to determine the line pipe fracture parameter $(CTOA)_{\max}$ are: the elasto-plastic dynamic-fracture computational model; full-scale pipe fracture experimentation; a small-scale characterization test.

As a result of the parametric study, an interpolation formula has been developed for pipeline steels, this is given by the general form:

$$CTOA_{\max} = C \left(\frac{\sigma_h}{E} \right)^m \left(\frac{\sigma_h}{\sigma_{flow}} \right)^n \left(\frac{D}{t} \right)^q \quad (1.11)$$

In which $(CTOA)_{\max}$ is the maximum steady-state crack driving force, σ_h refers to hoop stress in units of MPa, σ_{flow} refers to flow stress in units of MPa, m, n and q are dimensionless constants and C is in unit of degrees. These quantities are determined by fitting equation to the results of the parametric study. This exercise led to the following values of the constants for methane: C = 106; m = 0.753; n = 0.778; q = 0.65. The error of this interpolating

formula is within 8%.

1.6 Objectives of this thesis

1st. Overcome the limitations of classical Battelle-TCM in predicting high grade pipe toughness by deriving a new modified two-curve formula. In the past, only correction factors (section 1.3.3.1-1.3.3.3) and new constants (section 1.3.3.4) are manipulated to give better results of fracture toughness for high grade pipes, as compares to the original Battelle-TCM. We derive a new “Limit (crack) Speed” based two-curve method (LS-TCM) to give more accurate estimation of fracture toughness in some cases for both low and high grade pipes, as detailed in section 2.1.

2nd. Some formulas are derived for both single-curve method and two-curve method for DWTT energy. DWTT energy is frequently used in fracture toughness studies nowadays because DWTT specimen has a fracture path longer than CVN specimen to better characterize ductile fracture. However there has been no explicit formula for DWTT energy up until now. Some formulas for single-curve method for DWTT energy (DWTT-SCM) and two-curve method for DWTT energy (DWTT-TCM) are derived in chapter 3 to facilitate the usage of DWTT energy in future studies of fracture toughness.

3rd. Linear relationships between CVN-DWTT and CVN-CTOA are proposed in section 3.2 and 4.2, in order to give designer more choices in selecting parameters for fracture toughness studies, through correlating the relatively new toughness parameters DWTT energy and CTOA to the original toughness parameter CVN energy.

4th. Single curve formula for CVN energy and CTOA already exists in

literature to characterize low grade pipe toughness. However their applicability for high grade pipes were not well addressed. We discuss this issue in section 2.2 and 4.1.

Chapter 2

Analysis of Charpy V-Notch (CVN) energy

2.1 A “Limit Speed” based Two-curve Method (LS-TCM)

In this section we firstly use a database to derive the “Limit Speed” based two-curve method, then we manipulate this method to calculate the fracture toughness for both low and high grade pipes, and compares the calculated toughness to those resulted from Battelle-TCM and Higuchi-TCM.

2.1.1 Database for TCM calculation

8 data results are selected from other papers, characterizing pipe grades range from X52 to X120, especially high pipe grade X100 (4 data results belongs to grade X100), they will be manipulated in a series of calculations and derivations in section 2.1 :

① Pipe grade: X52, Diameter: 508mm, Thickness: 12mm, P_i :12.8MPa,

V_a :396m/s, At maximum speed: σ_{flow} :482.6MPa, C_v :32.5J, V_f :156m/s,

P_a :5.65MPa, P_d :8.78MPa,

At arrest toughness: σ_{flow} :482.6MPa, C_v :32.5J.

(P_i : the initial pressure in the pipe, V_a : the Acoustic velocity for natural gas

can be referred in [25]; acoustic velocity for air can be calculated using: $V_a =$

$331.5\text{m/s} + 0.6T$, σ_{flow} : flow stress, C_v : Charpy V-notch energy, V_f : crack

speed, P_a : arrest pressure, P_d : decompressed pressure at the crack tip.)

This is the result of 40 larger Athens experiments done at around 1969. Design temperature: -20 °C, pressurizing gas: natural gas [8].

□ Pipe grade: X70, Diameter: 1219.2mm, Thickness: 18.3mm, P_i :11.6MPa,
 V_a :370m/s,

At maximum speed: σ_{flow} :604MPa, C_v :51J, V_f :356m/s, P_a :3.61MPa,
 P_d :10.21MPa,

At arrest toughness: σ_{flow} :561MPa, C_v :188J.

This test is done in 1978 in Kamaishi, Japan, by High Strength Line Pipe Research Committee. The test materials were API 5LX X70 UOE pipes. The test pipes had a dimension of 48-in. diameter, 0.72-in. wall thickness and were mainly 10 m long. Test temp 3-12 °C, pressurizing gas: air [26].

□ Pipe grade: X70, Diameter: 1219.2mm, Thickness: 18.3mm, P_i :11.6MPa,
 V_a :370m/s,

At maximum speed: σ_{flow} :610MPa, C_v :76J, V_f :260m/s, P_a :4.18MPa,
 P_d :8.35MPa,

At arrest toughness: σ_{flow} :556MPa, C_v :126J.

This test is done in 1978 in Kamaishi, Japan, by High Strength Line Pipe Research Committee. The test materials were API 5LX X70 UOE pipes. The test pipes had a dimension of 48-in. diameter, 0.72-in. wall thickness and were mainly 10 m long. Test temp 3-12 °C, pressurizing gas: air [26].

□ Pipe grade: X100, Diameter: 1422.4mm, Thickness: 19.1mm, P_i :12.6MPa,
 V_a :343.5m/s,

At maximum speed: σ_{flow} :815.5MPa, C_v :151J, V_f :300m/s, P_a :5.01MPa,
 P_d :10.85MPa

At arrest toughness: σ_{flow} :712.5MPa, C_v :263J

This test is done in 1998 at the CSM Perdasdefogu Test Station in Sardinia, this project is carried out on behalf of ECSC (European Coal and Steel Community) by a joint co-operation among CSM, SNAM and Europipe. Full scale DWTT tests temp: 20 °C, pressurizing gas: air [27].

[5] Pipe grade: X100, Diameter: 914.4mm, Thickness: 16.0mm, P_i :18.1MPa,
 V_a :343.5m/s,

At maximum speed: σ_{flow} :755.5MPa, C_v :165J, V_f :310m/s, P_a :7.05MPa,
 P_d :16.14MPa

At arrest toughness: σ_{flow} :752MPa, C_v :297J

This test is done in 1998 at the CSM Perdasdefogu Test Station in Sardinia, this project is carried out on behalf of ECSC (European Coal and Steel Community) by a joint co-operation among CSM, SNAM and Europipe. Full scale DWTT tests temp: 20 °C, pressurizing gas: air [28].

[6] Pipe grade: X100, Diameter: 914.4mm, Thickness: 16.0mm, P_i :19.3MPa,
 V_a :495m/s,

At maximum speed: σ_{flow} :825MPa, C_v :183J, V_f :250m/s, P_a :7.57MPa,
 P_d :10.56MPa

At arrest toughness: σ_{flow} :761.5MPa, C_v :270J

This test is done at the Test Station in Perdasdefogu, Sardinia. Full scale DWTT tests temp: 14 °C, pressurizing gas: rich natural gas (methane > 98%)

[28].

[7] Pipe grade: X100, Diameter: 914.4mm, Thickness: 20.0mm, P_i :22.56MPa,

V_a :535m/s,

At maximum speed: σ_{flow} :758MPa, C_v :199J, V_f :255m/s, P_a :8.98MPa,

P_d :11.91MPa

At arrest toughness: σ_{flow} :765.5MPa, C_v :231J

This test is done at the Test Station in Perdasdefogu, Sardinia. Full scale

DWTT tests temp: 14 °C, pressurizing gas: rich natural gas (methane > 98%)

[29].

[8] Pipe grade: X120, Diameter: 914.4mm, Thickness:16.0mm, P_i :20.85MPa,

V_a :510m/s,

At maximum speed: σ_{flow} :879MPa, C_v :151J, V_f :350m/s, P_a :7.40MPa,

P_d :14.32MPa

At arrest toughness: σ_{flow} :879MPa, C_v :273J

This test was done in 2000 at Sardinia, Italy, by Centro Sviluppo Materiali

S.p.A. on behalf of ExxonMobil. Test pressure: 12 °C, pressurizing gas: natural

gas (98 % methane), no back fill [30].

2.1.2 Derivation of “Limit Speed” based Two-curve Method (LS-TCM)

A V-p relation is suggested according to theoretical investigations [31]:

$$V_f = V_{limit} \left(1 - \left[\frac{P}{P_a} \right]^{\frac{-2}{\delta}} \right) \quad (2.1)$$

Considering that V_{limit} is a constant for a given material, we assume

$$V_{limit} = \lambda \cdot \frac{\sigma_{flow}}{\sqrt{C_v}}, \text{ therefore we have the "Limit (crack) Speed" based two-curve}$$

method (LS-TCM) as follows. The reason for this method to be called "Limit Speed" can be traced from formula (2.1), where we can see that there is an upper speed limit V_{limit} for the crack speed, which means that, for a given material and pipe grade, the crack speeds never exceed a speed limit.

$$V_f = \lambda \cdot \frac{\sigma_{flow}}{\sqrt{C_v}} \left(1 - \left[\frac{P_d}{P_a} \right]^{\frac{2}{\delta}} \right) \quad (2.2)$$

There are two unknowns in this equation, λ and δ , we need to choose two data points, one is point [2] (because point [2] is the closest point to the trace of the anticipated crack speed curve among the three low position points [1], [2] and [3]), another from other 7 data points to solve this equation.

Try points [2] (356, 2.828) and [1] (156, 1.554),
 $\Rightarrow \lambda = 39.59, \delta = 18.5, -2 / \delta = -0.1081$

Sample calc:
$$\frac{1}{156} \cdot \frac{482.6}{\sqrt{32.5}} \cdot \left(1 - 1.554^{-\frac{2}{\delta}} \right) = \frac{1}{\lambda} = \frac{1}{356} \cdot \frac{604}{\sqrt{51}} \cdot \left(1 - 2.828^{-\frac{2}{\delta}} \right);$$

Try points [2] (356, 2.828) and [3] (260, 1.998),
 $\Rightarrow \lambda = 4.19, \delta = 0.64, -2 / \delta = -3.125$

Try points [2] (356, 2.828) and [4] (300, 2.166), $\Rightarrow \lambda, \delta = N / A$

Try points [2] (356, 2.828) and [5] (310, 2.289), $\Rightarrow \lambda, \delta = N / A$

Try points [2] (356, 2.828) and [6] (250, 1.395),
 $\Rightarrow \lambda = 4.21, \delta = 0.18, -2 / \delta = -11.111$

Try points [2] (356, 2.828) and [7] (255, 1.326), $\Rightarrow \lambda, \delta = N / A$

Try points [2] (356, 2.828) and [8] (350, 1.935), $\Rightarrow \lambda, \delta = N / A$

The condition for $\delta > 0$ (to ensure crack speed increases when decompressed pressure increases) is very complex, however according to above calculation we find a simple relation:

$$\frac{\sigma_{flow2}}{V_{f2} \sqrt{C_{v2}}} < \frac{\sigma_{flowx}}{V_{fx} \sqrt{C_{vx}}} \quad (2.3)$$

Data pair [1]-[2] give most reasonable crack speed when we put points [1] and [2] into eqn. (2.2), therefore we use these two data points to derive the general form of the LS-TCM formula:

$$\left\{ \begin{array}{l} V_f = 39.59 \cdot \frac{\sigma_{flow}}{\sqrt{C_v}} \left(1 - \left[\frac{P_d}{P_a} \right]^{-0.1081} \right) \\ \frac{P_d}{P_i} = \left[\frac{V_d}{6V_a} + \frac{5}{6} \right]^7 \\ P_a = \frac{4}{3.33\pi} \cdot \frac{t}{D} \cdot \sigma_{flow} \cdot \cos^{-1} \exp \left(\frac{-18.75 \cdot \pi E \cdot C_v}{24 \sqrt{Dt} / 2 \cdot \sigma_{flow}^2} \right) \end{array} \right. \quad (2.4)$$

2.1.3 Calculation of fracture toughness using LS-TCM

At intersection point of Battelle two-curve method (see Figure 2-1), we have:

$$V_f = V_d, \quad (2.5)$$

And $\frac{dV_f}{dP_d} = \frac{dV_d}{dP_d}, \quad (2.6)$

Put Eqn. (2.5)-(2.6) into the following Battelle-TCM:

$$\left\{ \begin{array}{l} V_f = 2.76 \times \frac{\sigma_{flow}}{\sqrt{C_v}} \times \left(\frac{P_d}{P_a} - 1 \right)^{\frac{1}{6}} \\ \frac{P_d}{P_i} = \left[\frac{V_d}{6V_a} + \frac{5}{6} \right]^7 \\ P_a = \frac{4}{3.33\pi} \cdot \frac{t}{D} \cdot \sigma_{flow} \cdot \cos^{-1} \exp \left(\frac{-18.75 \cdot \pi E \cdot C_v}{24 \sqrt{Dt} / 2 \cdot \sigma_{flow}^2} \right) \end{array} \right. \quad (2.7)$$

We can get:

$$V_f = 2.76 \times \frac{\sigma_{flow}}{\sqrt{C_v}} \times \left(\frac{P_i \left[\frac{V_f}{6V_a} + \frac{5}{6} \right]^7}{P_a} - 1 \right)^{\frac{1}{6}} \quad (2.8)$$

$$0.46 \times \frac{\sigma_{flow}}{\sqrt{C_v}} \times \frac{1}{P_a} \times \left(\frac{P_i \left[\frac{V_f}{6V_a} + \frac{5}{6} \right]^7}{P_a} - 1 \right)^{\frac{5}{6}} = \frac{6}{7} \cdot \frac{V_a}{P_i} \times \left(\frac{V_f}{6V_a} + \frac{5}{6} \right)^{-6} \quad (2.9)$$

There are two unknowns in Eqn. (2.8)-(2.9): V_f and C_v . Put pipe and pressure data for points [1] and [2] (from section 2.1.1) into Eqn. (2.8)-(2.9), use Matlab to calculate the fracture toughness for Battelle-TCM. Results are listed in Table 2-1.

Similarly, put Eqn. (2.5) and (2.6) into Eqn. (2.4), we have another two equations for LS-TCM:

$$V_f = \lambda \cdot \frac{\sigma_{flow}}{\sqrt{C_v}} \left(1 - \left[\frac{P_i \left[\frac{V_f}{6V_a} + \frac{5}{6} \right]^7}{P_a} \right]^{\frac{2}{\delta}} \right) \quad (2.10)$$

$$\frac{\lambda \cdot \frac{2}{\delta} \cdot \sigma_{flow}}{\sqrt{C_v}} \times \frac{1}{P_a} \times \left(\frac{P_i \left[\frac{V_f}{6V_a} + \frac{5}{6} \right]^7}{P_a} \right)^{-1-\frac{2}{\delta}} = \frac{6}{7} \cdot \frac{V_a}{P_i} \times \left(\frac{V_f}{6V_a} + \frac{5}{6} \right)^{-6} \quad (2.11)$$

Results of fracture toughness calculated by LS-TCM are listed in Table 2-1. There is also a comparison between Battelle-TCM and LS-TCM in Figure 2-1.

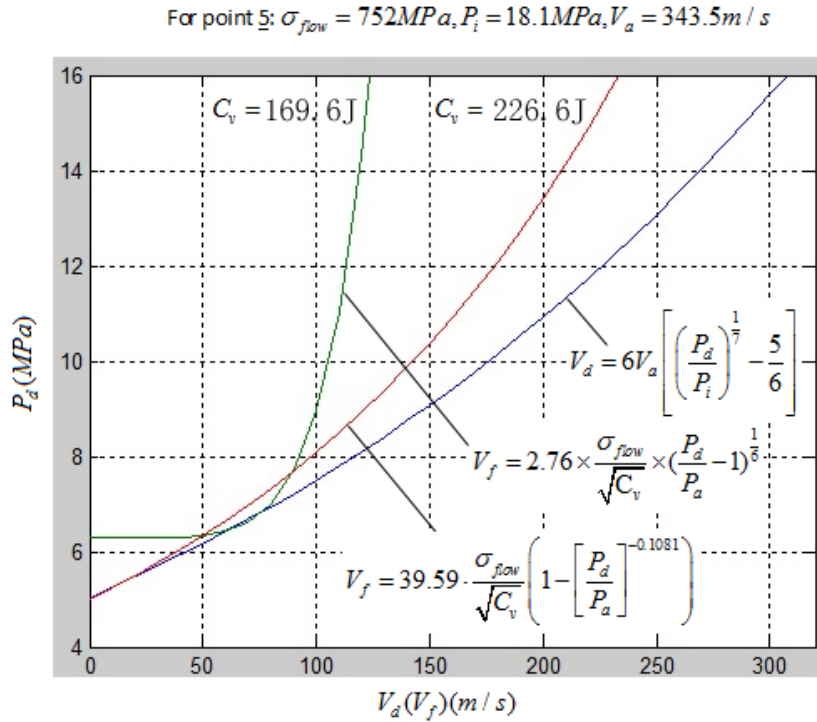


Figure 2-1 Sample comparison of two-curves for Battelle-TCM and LS-TCM

for data point [5].

For Higuchi-TCM (formula given in section 1.3.3.4) we have another two equations (2.12) and (2.13), similar to Eqn. (2.8) and (2.9), fracture toughness calculated by Higuchi-TCM is listed in Table 2-1. Fracture toughness calculated from the three two-curve methods are compared in Figure 2-2.

$$V_f = 10\alpha \times \frac{\sigma_{flow}}{\sqrt{C_v}} \times \left(\frac{P_i \left[\frac{V_f}{6V_a} + \frac{5}{6} \right]^7}{P_a} - 1 \right)^\beta \quad (2.12)$$

$$10\alpha\beta \cdot \frac{\sigma_{flow}}{\sqrt{C_v}} \times \frac{1}{P_a} \times \left(\frac{P_i \left[\frac{V_f}{6V_a} + \frac{5}{6} \right]^7}{P_a} - 1 \right)^{\beta-1} = \frac{6}{7} \cdot \frac{V_a}{P_i} \times \left(\frac{V_f}{6V_a} + \frac{5}{6} \right)^{-6} \quad (2.13)$$

Table 2-1 Fracture toughness calculated by different two-curve methods (σ_{flow} : flow stress, C_v : Charpy V-notch energy, P_i : initial pressure, V_a : acoustic speed)

	1	2	3	4	5	6	7	8
$\sigma_{flow} (MPa)$	482.6	561	556	712.5	752	761.5	765.5	879
$P_i (MPa)$	12.8	11.6	11.6	12.6	18.1	19.3	22.56	20.85
$V_a (m/s)$	396	370	370	343.5	343.5	495	535	510
Test toughness(J)	32.5	188	126	263	297	270	252	273
Battelle-TCM tough(J)	31.8	99.2	99.9	163.4	169.6	146.5	126.2	163.3
Arrest factor=1.63*	1.02	1.89	1.26	1.61	1.75	1.84	2.00	1.67
Maxey-SCM tough(J)	37.9	118.8	118.8	187.0	185.0	210.3	198.1	245.4
Arrest factor=1.19	0.86	1.58	1.06	1.41	1.61	1.28	1.27	1.11
Higuchi-TCM tough(J)	24.7	84.2	83.1	227.4	114.0	85.9	60.2	86.6
Arrest factor=2.42	1.32	2.26	1.52	1.16	2.61	3.14	4.19	3.15
LS-TCM tough $\left[\frac{2}{\beta} - \frac{1}{\beta} \right]$ (J)	31.7	146.1	110.7	249.9	226.6	230.0	267.3	283.3
Arrest factor=1.11	1.03	1.29	1.14	1.05	1.31	1.17	0.94	0.96

* Arrest factor=test toughness/predicted toughness

From Table 2-1 and Figure 2-2 we can see that, fracture toughness predicted by LS-TCM (average arrest factor equals to 1.11) for available data we cited in section 2.1.1 is better than Battelle-TCM (average arrest factor equals to 1.63). For X52 to X70 low grade pipes, the average arrest factor for LS-TCM is 1.14 and the average arrest factor for Battelle-TCM is 1.39. For X100 and X120 high grade pipes, the average arrest factor for LS-TCM is 1.09 and the average

arrest factor for Battelle-TCM is 1.77. Therefore, Battelle-TCM can still be used in toughness calculations for low grade pipes, while LS-TCM is suitable for high grade pipe toughness calculations.

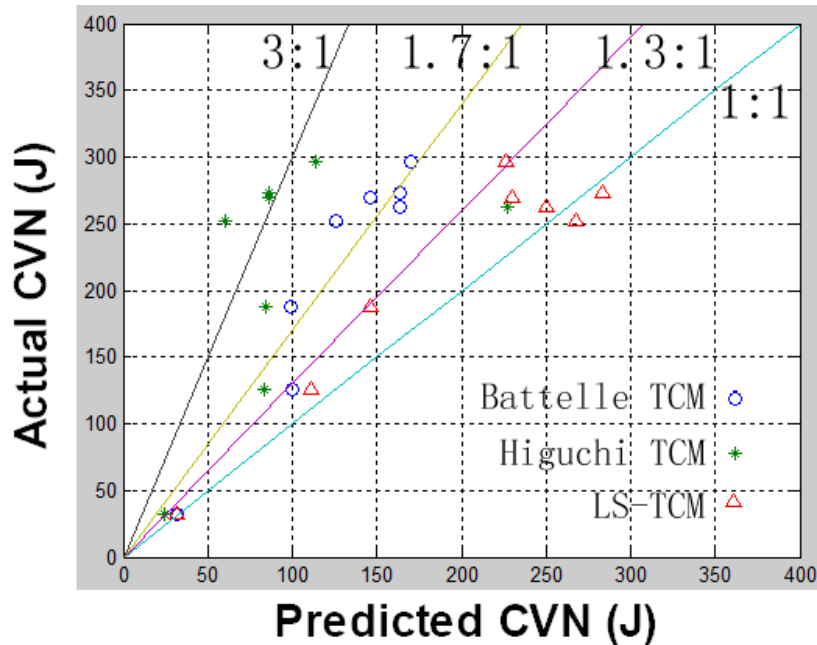


Figure 2-2 Fracture toughness calculated from three two-curve methods.

Arrest toughness given by Higuchi-TCM is worse than that given by Battelle-TCM and LS-TCM, furthermore, 7 out of 8 of the Higuchi-TCM toughness are not real numbers according to the calculation in Matlab. We therefore suggest that Higuchi-TCM be modified for calculations of fracture toughness.

The convergence of arrest toughness given by LS-TCM is poorer than Battelle-TCM, showing that the reliability of Battelle Formula in predicting arrest toughness is better than that in LS-TCM. For example, when initial toughness which is input into Matlab varies between 200J-300J, Battelle still gives same result toughness; while initial number given by LS-TCM can only vary between 50J-80J to give the same result toughness.

It's found that arrest toughness is very sensitive to constants in V-P equation. For example, in Battelle-TCM, when use $\alpha = 2.76$, the toughness we get perfectly matches the toughness predicted by other papers; however, while use $\alpha = 2$, the toughness deviates by 30-100J.

2.1.4 Calculation of crack speed using LS-TCM

Manipulating Battelle-TCM, LS-TCM and Higuchi-TCM (formulas (2.4), (2.10), (2.12)), we calculate different crack speeds and compares them with the crack speeds from field tests in Table 2-2.

Table 2-2 crack speed calculation (D: diameter, t: thickness, σ_{flow} : flow stress,

C_v : Charpy V-notch energy, P_i : initial pressure, P_a : arrest pressure, P_d :

decompressed pressure, V_a : acoustic speed):

	1	2	3	4	5	6	7	8
D(mm)	508	1219.2	1219.2	1422.4	914.4	914.4	914.4	914.4
t(mm)	12	18.3	18.3	19.1	16.0	16.0	20.0	16.0
$\sigma_{flow}(MPa)$	482.6	604	610	815.5	755.5	825	758	879
$C_v(J)$	32.5	51	76	151	165	183	199	151
$P_i(MPa)$	12.8	11.6	11.6	12.6	18.1	19.3	22.56	20.85
$P_a(MPa)$	5.65	3.61	4.18	5.01	7.05	7.57	8.98	7.40
$P_d(MPa)$	8.78	10.21	8.35	10.85	16.14	10.56	11.91	14.32
$P_d / P_a(MPa)$	1.554	2.828	1.998	2.166	2.289	1.395	1.326	1.935

$V_a (m/s)$	396	370	370	343.5	343.5	495	535	510
Test speed(m/s)	151.8	356	260	300	310	250	255	350
Battelle speed(m/s)	159.5	263.6	191.3	187.9	169.3	144.7	122.8	195.8
Higuchi speed(m/s)	356.2	443.3	314.0	320.6	309.7	290.5	276.8	390.3
Limit speed $\frac{2}{1}$ (m/s)	155.8	355.6	199.5	210.4	199.2	85.3	63.8	194.9

The comparison of crack speeds calculated from different methods and the real test speed are shown in Figure 2-3. The figure and the table above shows that, the accuracy of Higuchi-TCM in characterizing the crack speed of high grade pipes (points $\frac{4}{8}$) is higher than LS-TCM and Battelle-TCM for given data. This conclusion agrees well with the findings in paper [32], which indicates that, the crack speed calculated from Higuchi-TCM for high grade pipes is much more accurate than that from original Battelle-TCM.

Furthermore, the accuracy of LS-TCM in characterizing crack speeds for low grade pipes (points $\frac{1}{3}$) is higher than Higuchi-TCM and Battelle-TCM. Therefore, Battelle-TCM derived from X52 to X60 grade pipes cannot be applied for crack speed calculation for X70 pipes, while LS-TCM can be used to compensate this defect, so as to say, LS-TCM is not only better than Battelle-TCM in predicting fracture toughness but also has an advantage in predicting crack speeds.

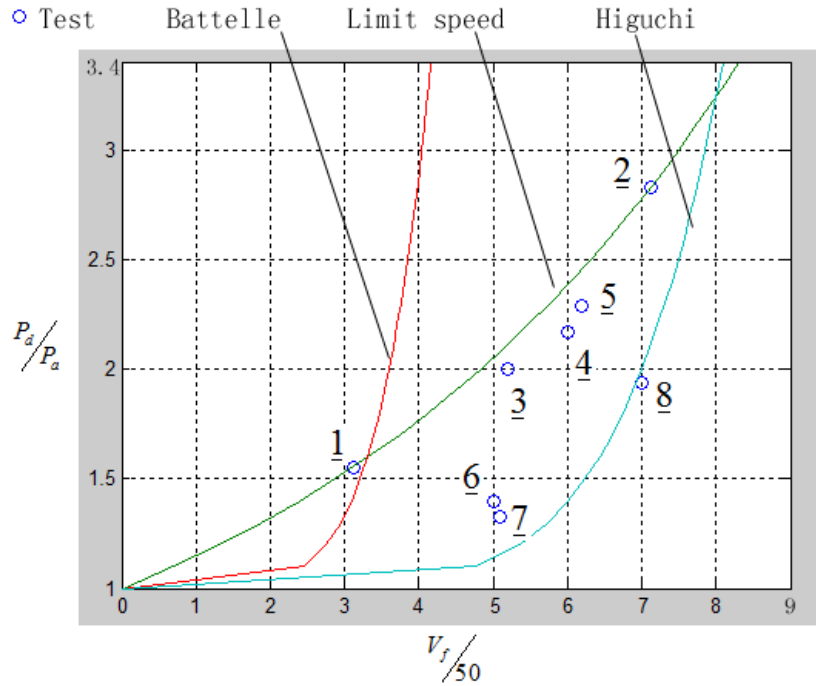


Figure 2-3 Comparison of calculated crack speed and test speed.

2.1.5 Modification to the Folias Factor

Folias correction factor is a function of $\frac{2c}{\sqrt{Rt}}$, it includes the influence of crack length into the following arrest pressure formula in Battelle-TCM:

$$P_a = \frac{4}{M_t \pi} \cdot \frac{t}{D} \cdot \sigma_{flow} \cdot \cos^{-1} \exp\left(\frac{-18.75 \cdot \pi E \cdot C_v}{24 \sqrt{Dt} / 2 \cdot \sigma_{flow}^2}\right) \quad (2.14)$$

Since for the high grade pipes the ratio of crack length to radius/thickness is changed, we tried to modify the Folias correction factor to see whether it better represents the fracture toughness for high grade pipes.

The expression for Folias Correction Factor is as follows [8]:

$$M_t = \left(1 + 1.255 \left(\frac{c}{\sqrt{Rt}} \right)^2 - 0.0135 \left(\frac{c}{\sqrt{Rt}} \right)^4 \right)^{\frac{1}{2}} \quad (2.15)$$

For low pipe grade, we take $\frac{c}{\sqrt{Rt}} = 3.0$ [9], and $M_t = 3.33$,

For X100, we take $\frac{c}{\sqrt{Rt}} = 1.56$ [10], and therefore $M_t = 1.99$.

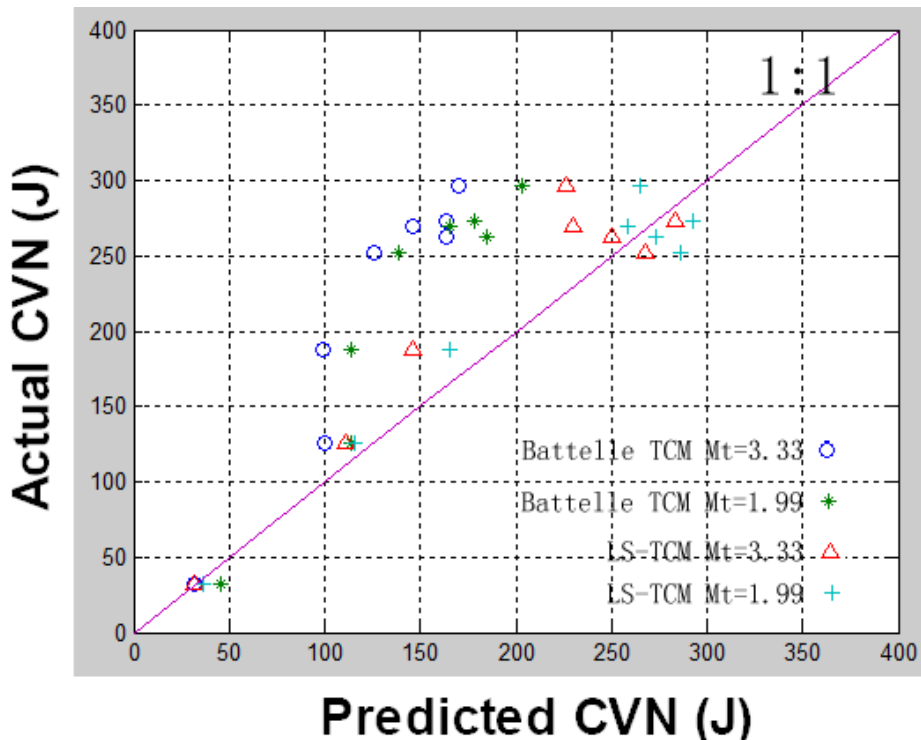


Figure 2-4 fracture toughness calculated using different Folias factors

The fracture toughness calculated using different Folias factors are listed in Table 2-3 and compared in Figure 2-4, both Battelle-TCM and LS-TCM are involved in this modification.

We can conclude from the results that, the modification of Folias factor better characterizes the fracture toughness for both low and high grade pipes, and enhances both Battelle-TCM and LS-TCM.

Table 2-3 fracture toughness calculated using different Folias factors

	1	2	3	4	5	6	7	8
Test toughness(J)	32.5	188	126	263	297	270	252	273
Battelle-TCM tough(J)	31.8	99.2	99.9	163.4	169.6	146.5	126.2	163.3
Folias factor=3.33	1.02	1.89	1.26	1.61	1.75	1.84	2.00	1.67
Battelle-TCM tough(J)	45.8	113.7	113.7	184.8	203.1	165.3	139.1	178.5
Folias factor=1.99	0.71	1.65	1.65	1.42	1.46	1.63	1.81	1.53
LS-TCM tough (J)	31.7	146.1	110.7	249.9	226.6	230.0	267.3	283.3
Folias factor=3.33	1.03	1.29	1.14	1.05	1.31	1.17	0.94	0.96
LS-TCM tough (J)	36.4	165.4	115.7	273.0	265.2	258.9	286.5	292.2
Folias factor=1.99	0.89	1.14	1.09	0.96	1.12	1.04	0.88	0.93

2.1.6 Remarks

From the analysis above, we find that the proposed LS-TCM is more accurate than Battelle-TCM in predicting arrest toughness for some known low/high grade pipe data, and also shows an advantage in calculating crack speed for low pipe grades.

The modification of Folias factor better characterizes the fracture toughness for both low and high grade pipes, and therefore could improve both Battelle-TCM and LS-TCM.

We discussed three two-curve methods (TCM) in this section, which TCM shall we choose for industrial line pipe design? We suggest that LS-TCM is probably suitable for fracture toughness calculations of high grade pipes and crack speed calculations of low grade pipes; Higuchi-TCM can be used to calculate crack speed for high grade pipes; on the other hand, Battelle-TCM is still applicable for fracture toughness calculations of low grade pipes.

2.2 Single-curve method (SCM)

2.2.1 Discussion about different single-curve methods

Several empirical single-curve methods developed to predict the two-thirds size CVN upper-shelf energies required for ductile fracture arrest are listed here [7]. Equations (2.16) through (2.19) summarize the approximate relationships including the original one developed by W. Maxey (Maxey-SCM). These SCM equations were derived by curve fitting pipe parameters and pressure data to the real CVN energies from experiments.

Original single-curve method developed by Maxey (Maxey-SCM) [33], same as eqn. (1.2):

$$C_{v-SCM-Maxey} = 0.709 \times 10^{-5} P_i^2 D^{2.333} t^{-1.667} \quad (2.16)$$

Single-curve method developed by AISI [34]:

$$C_{v-SCM-AISI} = 12.606 \times 10^{-5} P_i^{\frac{3}{2}} D^2 t^{\frac{3}{2}} \quad (2.17)$$

Single-curve method developed by Feanehough [35]:

$$C_{v-SCM-Feanehough} = 0.78 \times 10^{-3} P_i D^2 t^{\frac{3}{2}} - 0.315 \nu \times 10^{-3} P_i D^{\frac{9}{4}} t^{\frac{7}{4}} \quad (2.18)$$

$\nu = 0.396$ for natural gas

$\nu = 0.36$ for air

Single-curve method developed by Vogt [36]:

$$C_{v-SCM-Vogt} = 0.7452 \times 10^{-6} P_i^{2.33} D^{2.63} t^{-1.86} \quad (2.19)$$

Fracture toughness (CVN energy) calculated by the above four SCM equations are compared in Table. 2-4 and Figure 2-5. The average arrest factors for different SCM equations are:

Maxey-SCM: 1.19

AISI-SCM: 1.77

Feanehough-SCM: 2.00

Vogt-SCM: 1.09

In the past, Maxey-SCM is used as the standard SCM to calculate low grade pipe toughness. However, from the current data shown in Table 2-4 and Figure 2-5 we can see that, Vogt-SCM formula is better than Maxey-SCM and other single-curve methods in interpreting the toughness for high grade pipes. Therefore we take Maxey-SCM formula as the representative of the single-curve method formula, which will be used in the modification of SCM in latter section.

Table 2-4 fracture toughness calculated by different single-curve methods (D: diameter, t: thickness, P_i : initial pressure):

	1	2	3	4	5	6	7	8
	gas	air	air	air	air	gas	gas	gas
D (mm)	508	1219.2	1219.2	1422.4	914.4	914.4	914.4	914.4
t(mm)	12	18.3	18.3	19.1	16.0	16.0	20.0	16.0
P_i (MPa)	12.8	11.6	11.6	12.6	18.1	19.3	22.56	20.85
Test toughness(J)	32.5	188	126	263	297	270	252	273
Maxey-SCM tough(J)	37.9	118.8	118.8	187.0	185.0	210.3	198.1	245.4
Arrest factor	0.86	1.58	1.06	1.41	1.61	1.28	1.27	1.11
AISI-SCM toughness(J)	35.8	94.6	94.6	136.7	126.8	139.6	126.3	156.8
Arrest factor	0.91	1.99	1.33	1.92	2.34	1.93	2.00	1.74
Feanehough-SCM tough(J)	36.7	100.4	100.4	136.5	110.7	110.2	96.1	119.0
Arrest factor	0.89	1.87	1.25	1.93	2.68	2.45	2.62	2.29
Vogt-SCM tough (J)	36.4	132.0	132.0	221.7	224.3	260.5	247.4	311.8
Arrest factor	0.89	1.42	0.95	1.19	1.32	1.04	1.02	0.88

* Arrest factor=test toughness/predicted toughness

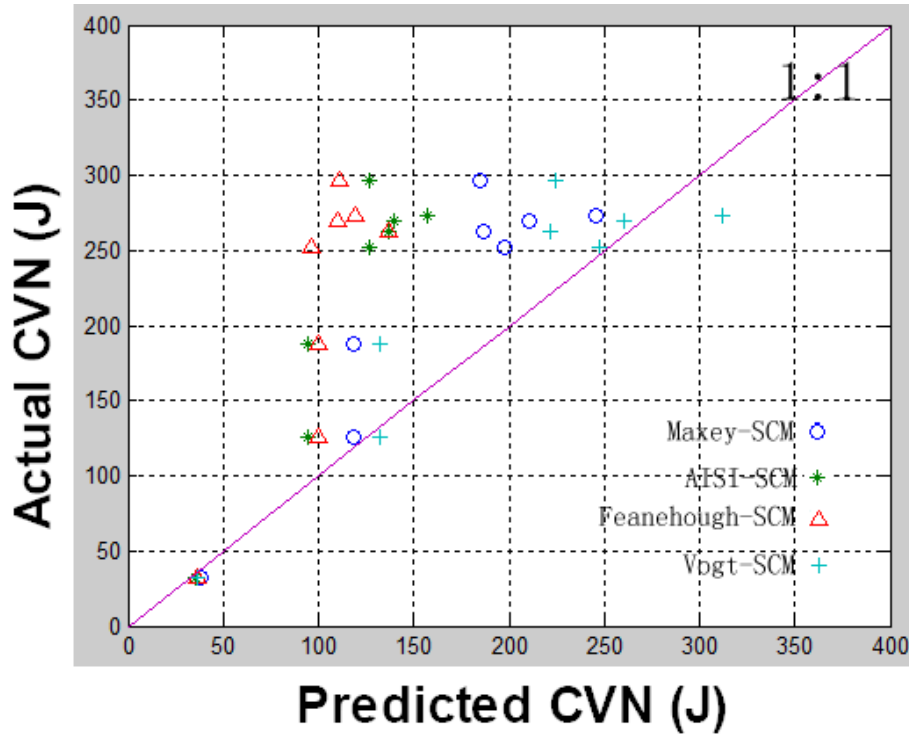


Figure 2-5 fracture toughness calculated by different single-curve methods.

2.2.2 Modifications to single-curve method developed by Vogt (Vogt-SCM)

We provide two ways to modify Vogt-SCM, one is to modify the constant only; another is to modify the index for pressure, diameter and thickness, besides the modification of constant.

Result for modification method I:

$$C_{v-Vogt-SCM-I} = 0.78 \times 10^{-6} P_i^{2.33} D^{2.63} t^{-1.86} \quad (2.20)$$

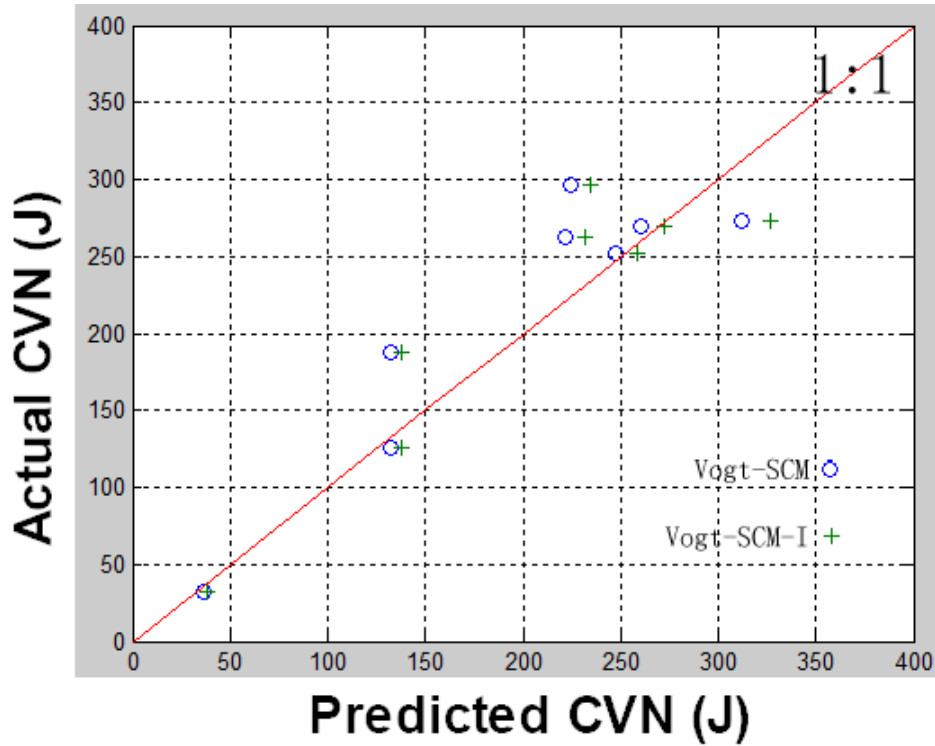


Figure 2-6 Result for modification method I for Vogt-SCM.

Results for modification Method II: Choose four points to fit the curve of formula $C_{v-Vogt-SCM-II} = a \times P_i^b D^c t^d$:

Choose points [1], [3], [6], [7] (Consider both low and high grade pipes):

$$C_{v-Vogt-SCM-II} = 1.78 \times 10^{-7} P_i^{2.55} D^{2.84} t^{-2.09} \quad (2.22)$$

Choose points [4], [6], [7], [8] (Consider high grade pipes only):

$$C_{v-Vogt-SCM-II} = 220.0 \times P_i^{0.065} D^{0.146} t^{-0.355} \quad (2.23)$$

The fit of points [4], [6], [7], [8] is not very good, due to the small range of toughness for these points.

From the modifications above we can see that, the original Vogt-SCM is accurate enough for predicting toughness for both low and high pipe grades, no further modification is required to characterize high grade pipe toughness.

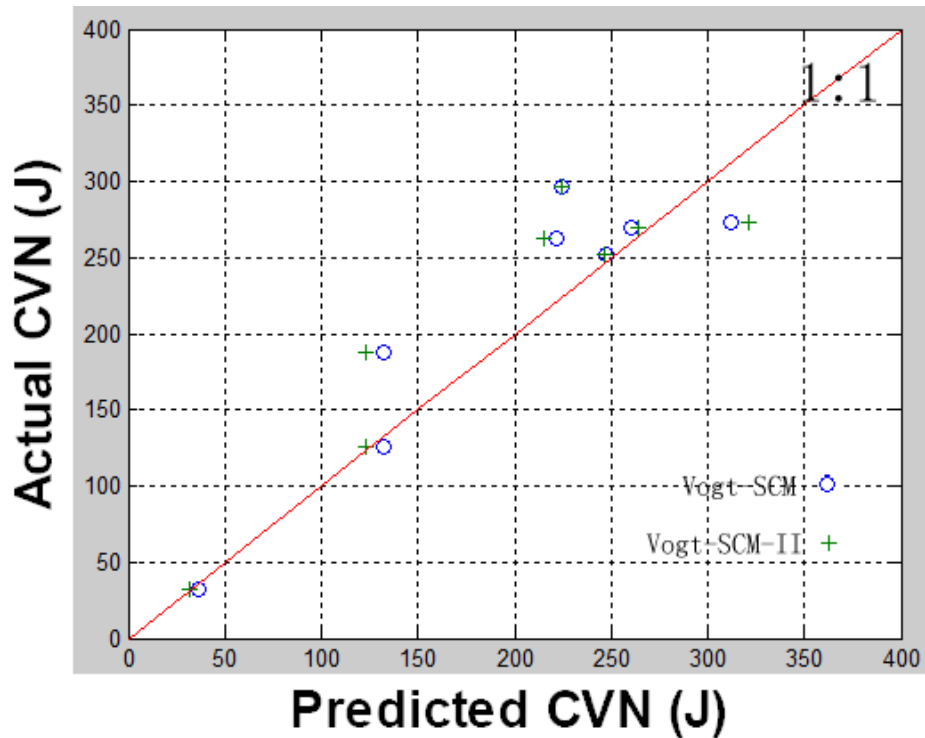


Figure 2-7 Result for modification method II for Vogt-SCM.

2.2.3 Comparison between Battelle-TCM and Maxey-SCM

Why the Battelle-TCM contains more input parameters than Maxey-SCM, but gives no better result than Maxey-SCM in predicting fracture toughness? This may be due to the fact that Maxey-SCM is intended to calculate the toughness only, but Battelle-TCM also calculates some dependent mechanical parameters other than the toughness.

In Maxey-SCM, there are 3 input parameters: D, t, P_i , 1 equation and 1 unknown: C_v .

$$C_v = 0.7452 \times 10^{-6} P_i^{2.33} D^{2.63} t^{-1.86}$$

While we have a relation between P_i and σ_{flow} :

$$P_i = \sigma_H \times \frac{2t}{D} = \frac{\sigma_{flow}}{M_T} \times \frac{2t}{D}, \quad (2.24)$$

where Folias Correction Factor $M_T = \left(1 + 1.255 \left(\frac{c}{\sqrt{Rt}}\right)^2 - 0.0135 \left(\frac{c}{\sqrt{Rt}}\right)^4\right)^{\frac{1}{2}}$

$$(2.25)$$

Therefore, σ_{flow} can be converted to P_i if we know the half length of the axial through-wall flaw c .

In Battelle-TCM, there are 5 input parameters: $D, t, P_i, \sigma_{flow}, V_a$, 5 equations and 5 unknowns: P_d, P_a, V_d, V_f and C_v .

$$\left\{ \begin{array}{l} V_f = 2.76 \times \frac{\sigma_{flow}}{\sqrt{C_v}} \times \left(\frac{P_d}{P_a} - 1\right)^{\frac{1}{6}} \\ \frac{P_d}{P_i} = \left[\frac{V_d}{6V_a} + \frac{5}{6}\right]^7 \\ P_a = \frac{4}{3.33\pi} \cdot \frac{t}{D} \cdot \sigma_{flow} \cdot \cos^{-1} \exp\left(\frac{-18.75 \cdot \pi E \cdot C_v}{24\sqrt{Dt} / 2 \cdot \sigma_{flow}^2}\right) \\ V_f = V_d \\ \frac{dV_f}{dP_d} = \frac{dV_d}{dP_d} \end{array} \right. \quad (2.26)$$

Parameter V_a which includes the gas properties in Battelle-TCM is determined from P_i , natural gas composition and test temperature, natural gas composition and test temperature are not considered in Maxey-SCM.

Battelle-TCM also calculates some dependent mechanical parameters, including P_d, P_a, V_d and V_f .

Therefore, pressurization conditions, pipe geometry, flow stress (crack length),

gas composition, test temperature are all included as input parameters in Battelle-TCM, while Maxey-SCM only considers pressurization conditions and pipe geometry.

Wilkowski [13] concludes in his paper that the accuracy of Battelle-TCM is a little better than Maxey-SCM for high grade pipes, This is not surprising since Maxey-SCM was empirically determined from the analysis on relatively low toughness pipes under lower pressure conditions.

However our data shows that under higher pressure conditions, and when average pipe grade is higher, the accuracy of Maxey-SCM is better than Battelle-TCM. Furthermore, our result shows the same trend as in paper [13], in which the accuracy of Maxey-SCM is worth than CSM-TCM [14] and Wilkowski-TCM [13]:

Maxey-SCM, average arrest factor: 1.19.

Battelle-TCM, average arrest factor: 1.63.

CSM-TCM toughness (section 1.3.3.1), average arrest factor: 1.17

$$C_{v-TCM-CSM} = 1.7C_{v-TCM} \quad (1.18)$$

Wilkowski-TCM toughness (section 1.3.3.3), average arrest factor: 0.95

$$C_{v-TCM-Wilkowski} = 0.056(0.1018C_{v-TCM} + 10.29)^{2.597} - 16.8 \quad (1.20)$$

Table 2-5 fracture toughness calculated by different methods (P_i : initial pressure):

	1	2	3	4	5	6	7	8
$P_i(MPa)$	128	116	116	126	181	193	2256	2085

Test toughness(J)	32.5	188	126	263	297	270	252	273
Maxey-SCM tough(J)	37.9	118.8	118.8	187.0	185.0	210.3	198.1	245.4
arrest factor	0.86	1.58	1.06	1.41	1.61	1.28	1.27	1.11
Battelle-TCM tough(J)	31.8	99.2	99.9	163.4	169.6	146.5	126.2	163.3
arrest factor	1.02	1.89	1.26	1.61	1.75	1.84	2.00	1.67
CSM-TCM tough(J)	44.5	138.9	139.9	228.8	237.4	205.1	176.7	228.6
arrest factor	0.73	1.35	0.90	1.15	1.25	1.32	1.43	1.19
Wilkowski-TCM tough(J)	31.9	146.0	147.6	346.0	370.7	283.6	218.1	345.6
arrest factor	1.02	1.29	0.85	0.76	0.80	0.95	1.16	0.79

* Arrest factor=test toughness/predicted toughness

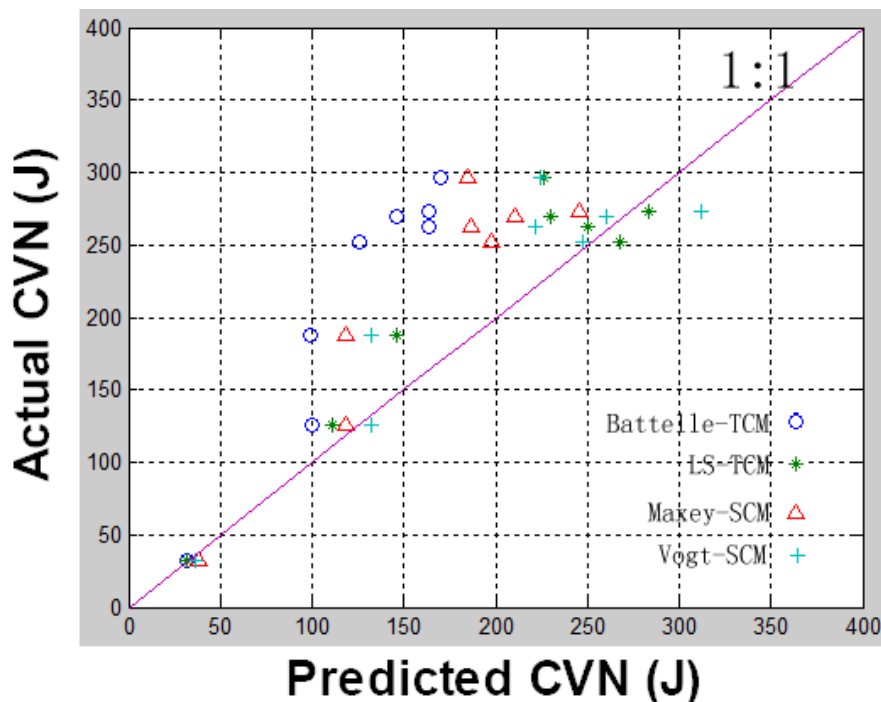


Figure 2-8 Vogt-SCM and LS-TCM both improves the fracture toughness

calculation of original Battelle-TCM and Maxey-SCM .

2.2.4 Remarks

We know that Battelle-TCM has been successful in calculating fracture toughness for low grade pipes, it gives predictions about crack propagation, crack arrest, crack velocity and so on. Maxey-SCM is another widely adopted method in predicting low grade pipe toughness because it is very simple.

Now when we consider the case of high grade pipes, we find that Vogt-SCM gives reasonable predictions of fracture toughness for current high grade pipe data, while original Maxey-SCM is shown to be non-conservative (see Figure 2-8).

When comparing the single-curve method and two-curve method for high grade pipe CVN energy calculation, we find that Vogt-SCM and the proposed LS-TCM have different advantages. Vogt-SCM gives reasonable predictions of high grade pipe CVN energy and is easy for calculation. On the other hand, the proposed LS-TCM results in accurate CVN energy for both low and high grade pipes, and is consistent with some fracture mechanics theories.

Chapter 3

Analysis of Drop-weight Tear Test (DWTT) energy

3.1 Derivation of DWTT Single-curve Method (DWTT-SCM)

Wilkowski mentioned in his paper [13] that Charpy-based fracture toughness criteria are grade sensitive, while DWTT energy predictions are not, but no detailed explanation was given.

We reviewed single-curve formula for both CVN and CTOA, and the database for DWTT energy, find that it is possible to introduce a single-curve formula for DWTT energy.

We first compare the range of CVN, CTOA and DWTT energy at different pipe grades, see Table 3-1.

Table 3-1 range of CVN, CTOA and DWTT energy at different pipe grades

	X60	X65	X70	X80	X100
CVN (ft-lb/in ²)	230-430	250-900	500-1200	550-1200	800-2200
CTOA (degree)	5 (X52)	/	10-11	10-14	14
DWTT (ft-lb/in ²)	900-1700	850-2500	1400-3300	1700-3700	1900-3900

From the table above, we can see that DWTT energy increases gradually with pipe grade, this trend is similar to that of CVN and CTOA.

Due to the linear relation between DWTT and CVN, we try to create a DWTT formula close to the form of the single-curve method formula (Vogt-SCM) for CVN:

$$C_{v-SCM-Vogt} = 0.7452 \times 10^{-6} P_i^{2.33} D^{2.63} t^{-1.86} \quad (2.20)$$

Then we collect data for DWTT and list them in Table 3-2, try to derive a single curve formula for DWTT energy.

Table 3-2 data for deriving SCM for DWTT energy (P_i : initial pressure, D: diameter, t: thickness, $DWTT_{pre}$: DWTT energy predicted by eqn.(3.1),

$DWTT_{exp}$: DWTT energy data from experiment [37]):

$P_i(MPa)$	D(mm)	t(mm)	$DWTT_{pre}(ft-lb)$	$DWTT_{exp}(ft-lb)$	Error(%)
6.9	762.0	8.7	973	1280	24.0
7.0	1219.2	11.7	1995	2000	0.2
8.9	1219.2	15.9	1974	2100	6.0
9.4	1066.8	12.4	2505	2300	8.9
9.9	1219.2	15.7	2590	3200	19.1
13.6	914.0	13.0	3613	3394	6.5
18.0	914.0	15.0	5320	4800	10.8

We does not change the form of the single-curve CVN formula but only change the constant in eqn.(2.20), finding that a new constant 1.59×10^{-5} gives the minimum error relative to experimental data of the DWTT energy.

$$DWTT_{SCM} = 1.59 \times 10^{-5} P_i^{2.33} D^{2.63} t^{-1.86} \quad (3.1)$$

The resultant prediction error for all 7 data series is about 10 percent (10.8%), within acceptable range. Curve fitting of eqn. (3.1) is also shown in Figure 3-1

The linear relation between DWTT energy and CVN energy already exists in literature [13]. Therefore we can manipulate the linear relation to validate the derivation of DWTT single-curve method from Vogt-SCM.

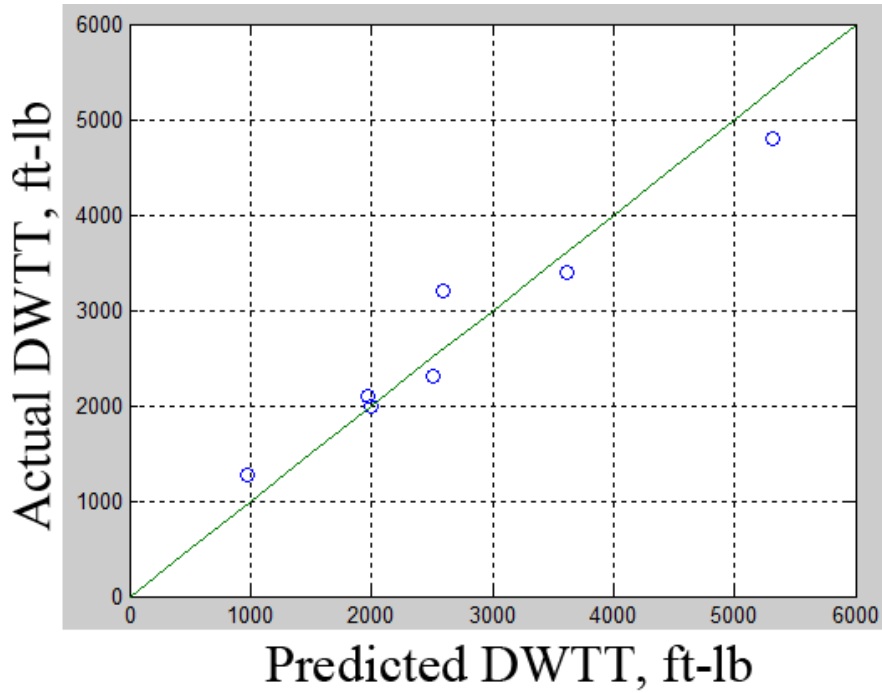


Figure 3-1 Curve fitting of result of DWTT-SCM to experiment data.

Manipulating the Vogt-SCM formula, we calculated the predicted CVN using data in Table 3-3, and compared it with the predicted DWTT energy to see if there exists a constant for the equation below:

$$DWTT_{SCM} = \text{const} \tan t * C_{v-Vogt-SCM} + 300, ft - lb / in^2 \quad (3.2)$$

From Table 3-3 and Figure 3-2 we can see that, the constant we get from eqn.(3.2) for both low and high grade pipes is close to the constant we can find in previous study (the constant is 3 in reference [8]) for low grade pipes,

$$DWTT_{SCM} = 3 * C_{v-Vogt-SCM} + 300, ft - lb / in^2 \quad (3.3)$$

Therefore it is reasonable to use the DWTT-SCM which derives from Vogt-SCM.

Table 3-3 comparison of predicted DWTT-SCM results and predicted Vogt-SCM results (P_i : initial pressure, D: diameter, t: thickness, $DWTT_{pred}$: DWTT energy predicted by eqn.(3.1), CVN_{pred} : CVN energy data predicted by eqn.(2.20)):

P_i (MPa)	D(mm)	t(mm)	$DWTT_{pred}$ (ft-lb)	CVN_{pred} (ft-lb)	Constant
6.9	762.0	8.7	973	183	3.68
7.0	1219.2	11.7	1995	571	2.97
8.9	1219.2	15.9	1974	558	3.00
9.4	1066.8	12.4	2505	708	3.11
9.9	1219.2	15.7	2590	732	3.13
13.6	914.0	13.0	3613	1034	3.20
18.0	914.0	15.0	5320	1523	3.30

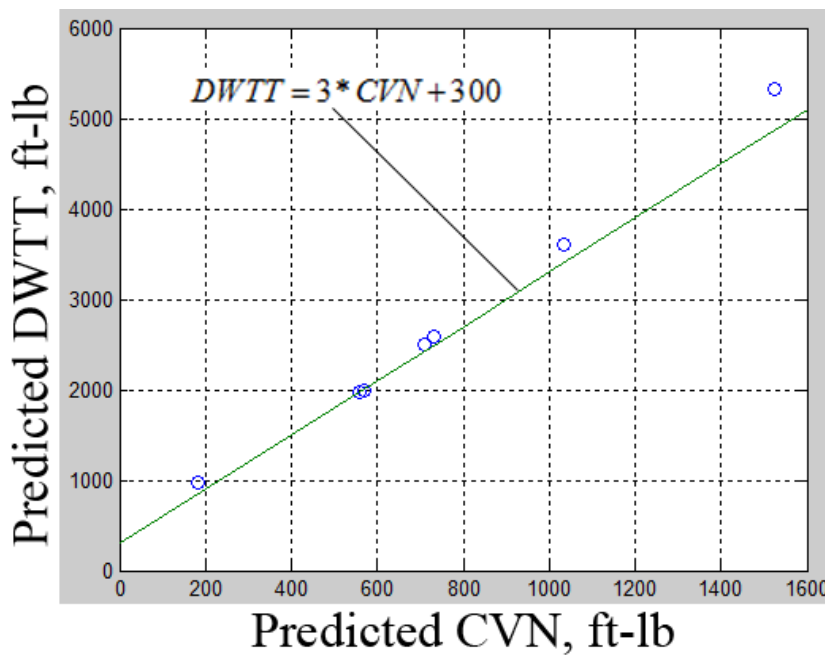


Figure 3-2 Curve fitting of the results in Table 3-3 to the equation from reference [37].

3.2 Discussion about the linear relation between DWTT and CVN energy

In the middle 1970's, Wilkowski first revealed a simple linear relationship between DWTT energy and CVN energy for low grade pipes [13]:

$$DWTT = 3 * CVN + 300, ft - lb / in2 \quad (3.4)$$

Later, considering the measurement of fracture propagation energy, he gave a non-linear relationship between DWTT energy and CVN as follows [37]:

$$DWTT = ((3 * CVN + 1800) / 175)^{2.5974}, ft - lb / in2 \quad (3.5)$$

Recently, Wilkowski found that the constant in the linear relationship changed when pipe grade increases [37], but there is no clear trend of how this constant changes. The challenge is that, is it true to use a linear formula to describe the relation between DWTT energy and CVN for different grade of pipes? Or in other words, which one better describes the relation between DWTT energy and CVN, the linear or non-linear formula? This section is purposed to answer the above questions.

We first take a look at the changes of the constant in Wilkowski's linear formula when pipe grade increases. The results are shown from Figure 3-3 to Figure 3-7. We notice that the correction factor increases when pipe grade increases, therefore the accuracy of the linear formula decreases when pipe grade increases.

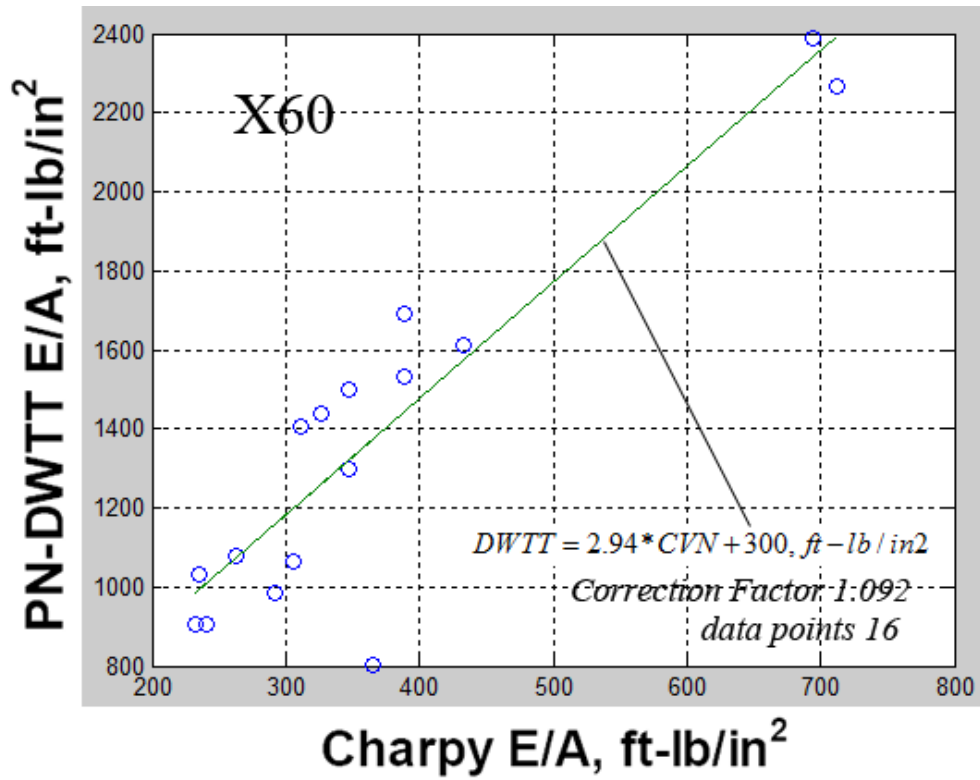


Figure 3-3 The linear ratio of DWTT/CVN for X60.

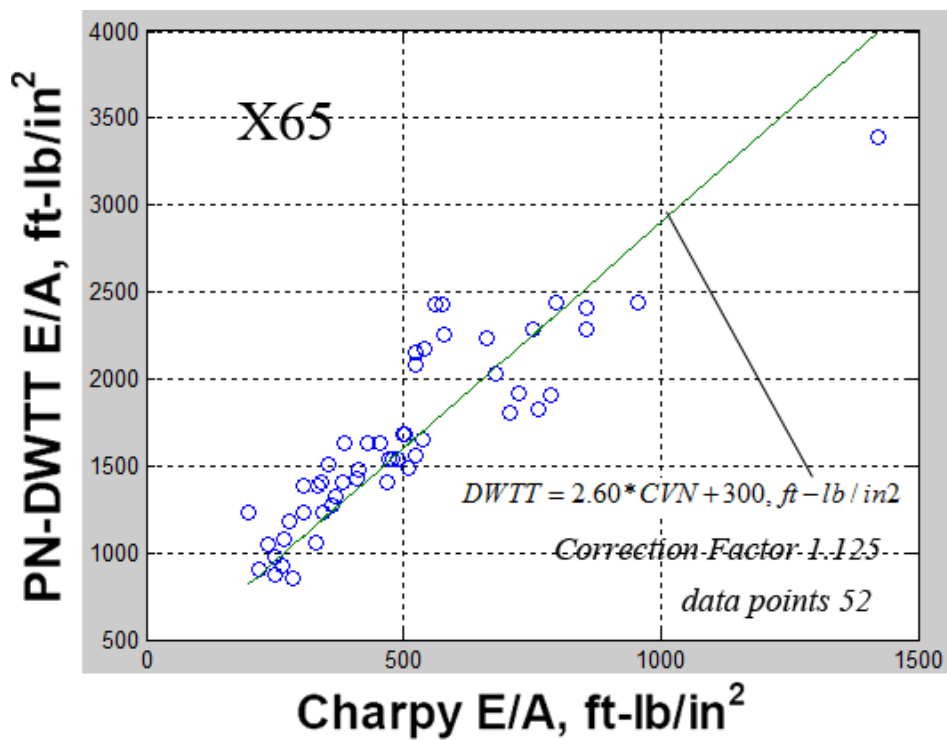


Figure 3-4 The linear ratio of DWTT/CVN for X65.

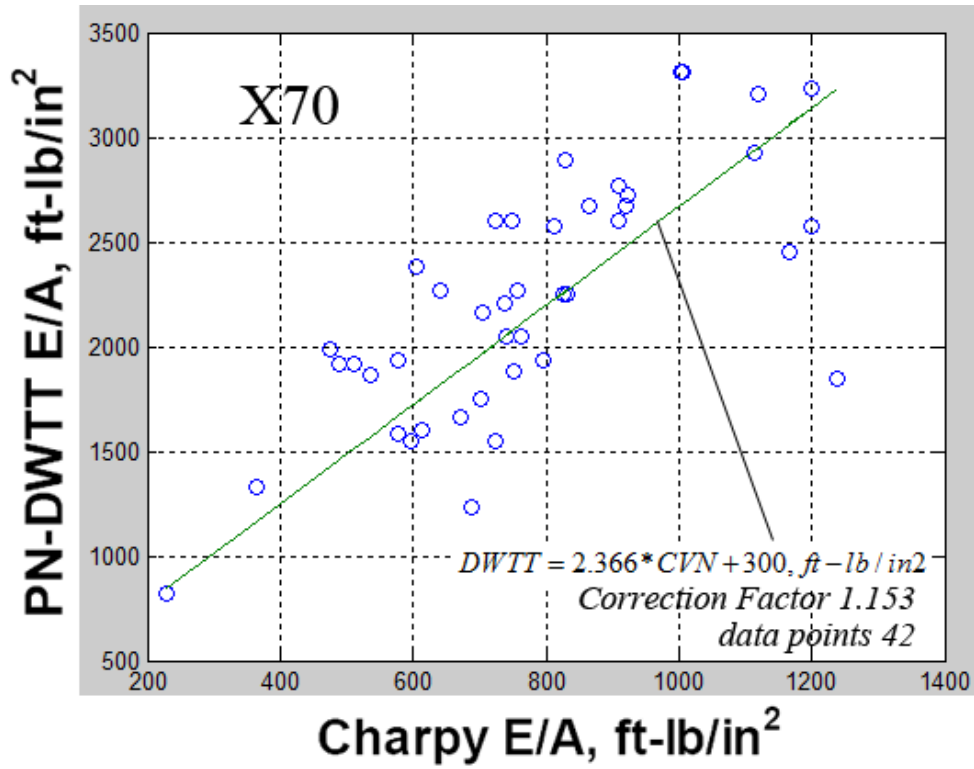


Figure 3-5 The linear ratio of DWTT/CVN for X70.

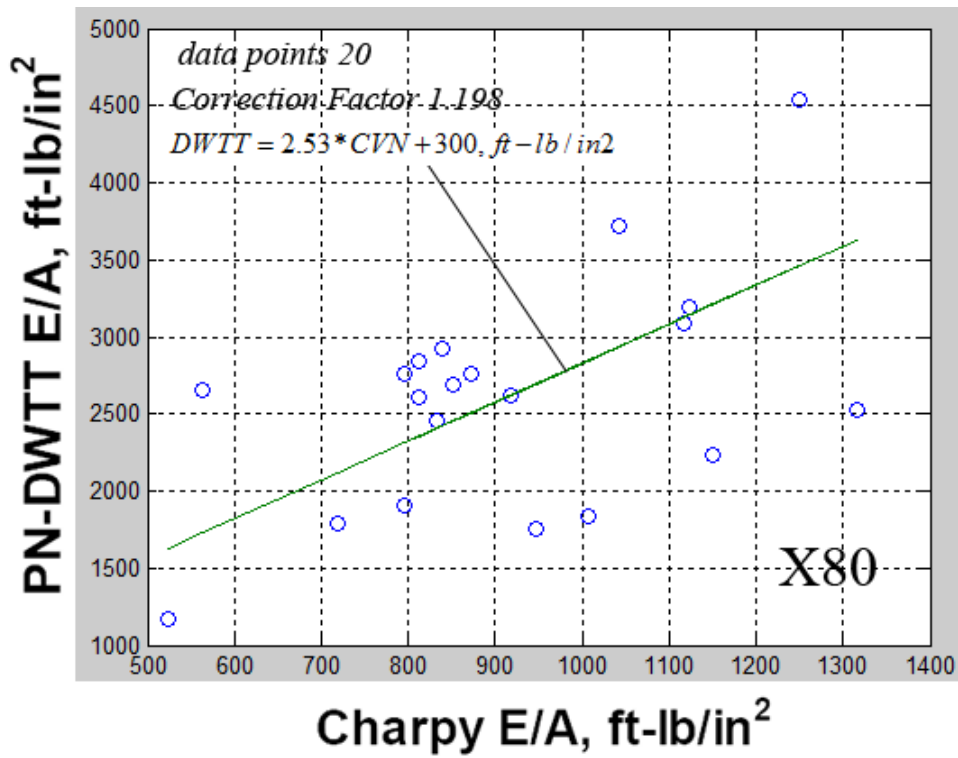


Figure 3-6 The linear ratio of DWTT/CVN for X80.

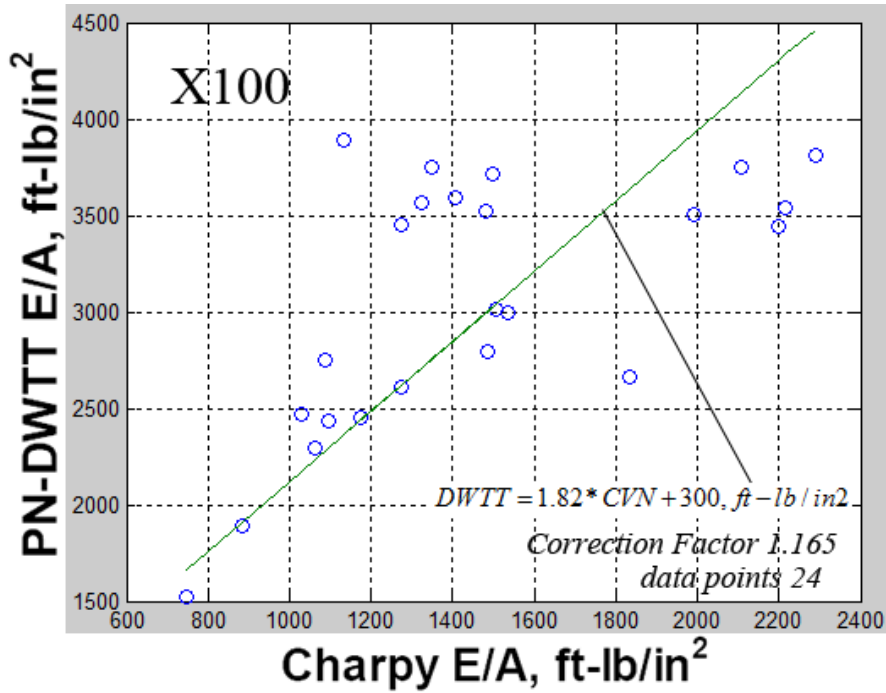


Figure 3-7 The linear ratio of DWTT/CVN for X100.

Non-linear formulas are also manipulated for different pipe grades to be compared with linear formulas. Result shown from Figure 3-8 to Figure 3-12.

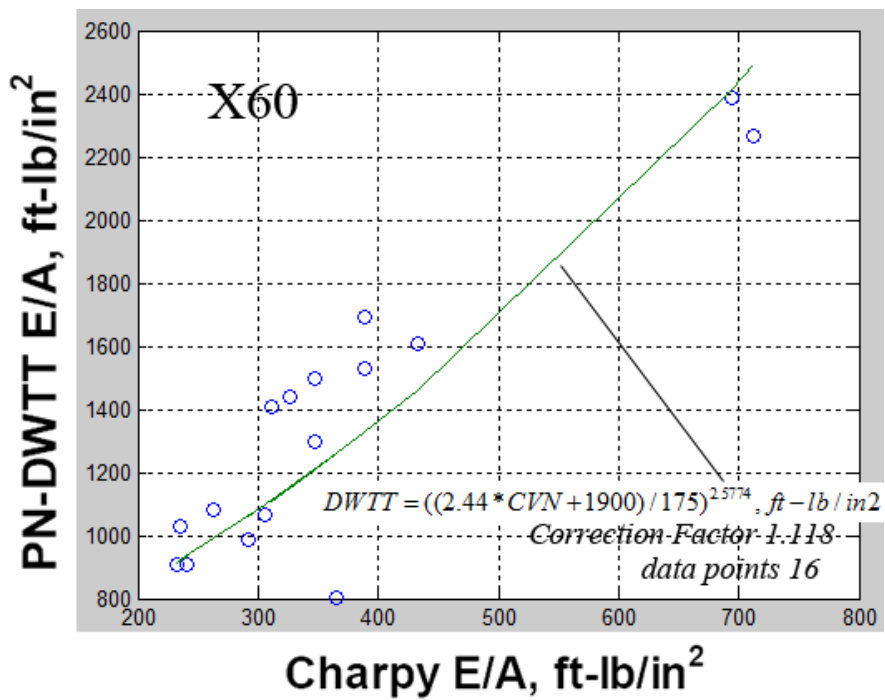


Figure 3-8 The non-linear ratio of DWTT/CVN for X60.

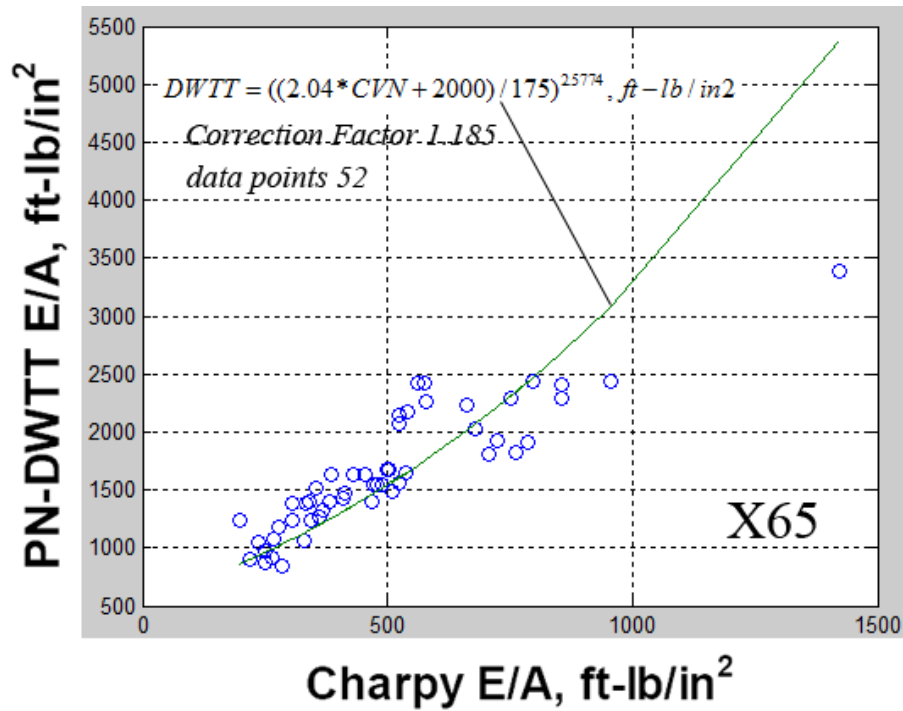


Figure 3-9 The non-linear ratio of DWTT/CVN for X65.

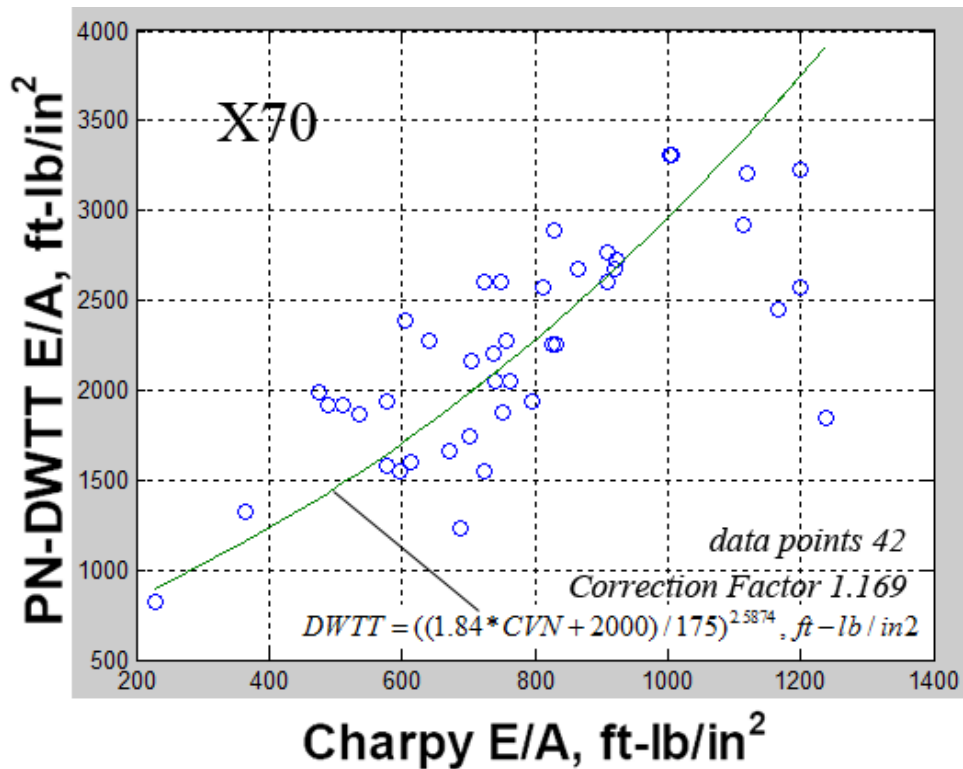


Figure 3-10 The non-linear ratio of DWTT/CVN for X70.

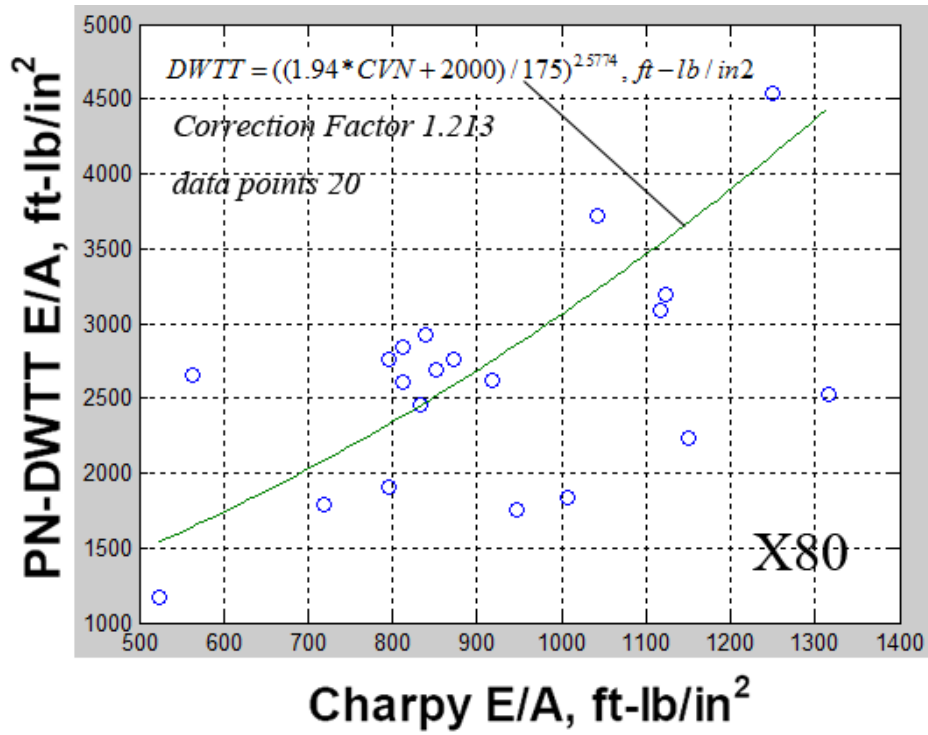


Figure 3-11 The non-linear ratio of DWTT/CVN for X80.

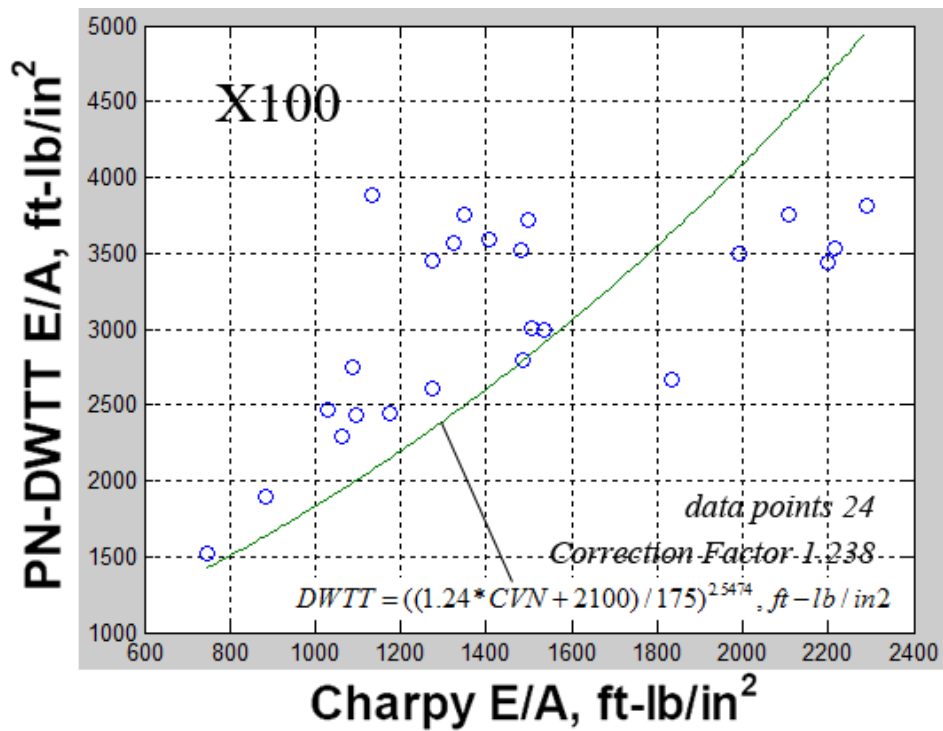


Figure 3-12 The non-linear ratio of DWTT/CVN for X100.

The linear formulas:

$$X 60, DWTT = 2.94 * CVN + 300, ft - lb / in2, correction, 1.092 \quad (3.6)$$

$$X 65, DWTT = 2.60 * CVN + 300, ft - lb / in2, correction, 1.125 \quad (3.7)$$

$$X 70, DWTT = 2.366 * CVN + 300, ft - lb / in2, correction, 1.153 \quad (3.8)$$

$$X 80, DWTT = 2.53 * CVN + 300, ft - lb / in2, correction, 1.198 \quad (3.9)$$

$$X 100, DWTT = 1.82 * CVN + 300, ft - lb / in2, correction, 1.165 \quad (3.10)$$

The non-linear formulas:

$$X 60, DWTT = ((2.44 * CVN + 1900) / 175)^{2.5774}, ft - lb / in2, correction, 1.118 \quad (3.11)$$

$$X 65, DWTT = ((2.04 * CVN + 2000) / 175)^{2.5774}, ft - lb / in2, correction, 1.185 \quad (3.12)$$

$$X 70, DWTT = ((1.84 * CVN + 2000) / 175)^{2.5874}, ft - lb / in2, correction, 1.169 \quad (3.13)$$

$$X 80, DWTT = ((1.94 * CVN + 2000) / 175)^{2.5774}, ft - lb / in2, correction, 1.213 \quad (3.14)$$

$$X 100, DWTT = ((1.24 * CVN + 2100) / 175)^{2.5474}, ft - lb / in2, correction, 1.238 \quad (3.15)$$

The comparison between linear and non-linear formulas shows that, linear formulas has a low prediction error and therefore better characterize the relation between DWTT energy and CVN.

Furthermore, from both linear and non-linear formulas we can see that, when pipe grade increases, the constant in the DWTT-CVN formula decreases, while the prediction error increases. This result agrees well with the conclusion in reference [13], and gives us a clear picture of the influence of pipe grade on

DWTT-CVN relationship.

3.3 Derivation of TCM expressed with DWTT energy (DWTT-TCM)

Manipulating the linear relationship (Eqn. (3.6)-(3.10)) between DWTT energy and CVN energy, we derive a series of new TCM formulas expressed with DWTT energy:

$$\left\{ \begin{array}{l} V_f = 2.76 \times \frac{\sigma_{flow}}{\sqrt{a^*(DWTT-300)}} \times \left(\frac{P_d}{P_a} - 1 \right)^{\frac{1}{6}} \\ \frac{P_d}{P_i} = \left[\frac{V_d}{6V_a} + \frac{5}{6} \right]^7 \\ P_a = \frac{4}{3.33\pi} \cdot \frac{t}{D} \cdot \sigma_{flow} \cdot \cos^{-1} \exp \left(\frac{-18.75 \cdot \pi E \cdot a^*(DWTT-300)}{24\sqrt{Dt} / 2 \cdot \sigma_{flow}^2} \right) \end{array} \right. \quad (3.16)$$

Where, For X60, a=0.34

For x65, a=0.38

For X70, a=0.42

For X80, a=0.40

For X100, a=0.55

The accuracy of this formula is as same as the classical TCM characterized with Charpy energy, therefore worse than that of the DWTT-SCM:

3.4 Remarks

In section 3.1, the SCM for DWTT energy, DWTT-SCM is proposed, a linear relationship is proposed between the DWTT energy calculated using DWTT-SCM and the CVN energy calculated using Vogt-SCM, which proves that the DWTT-SCM is successful as compared to available low/high grade pipe toughness data, and may be considered for high strength steel pipe

DWTT energy calculations in the future.

In section 3.2, the relationship between DWTT energy and CVN energy is considered, the comparison between linear and non-linear formula give us a clue that, linear formula better characterize the relation between DWTT energy and CVN, however the constant in the linear DWTT-CVN formula decreases when pipe grade increases.

In section 3.3, a new TCM is derived based on the linear relation between DWTT and CVN, so as to be called the DWTT-TCM. Manipulating the new DWTT-SCM and DWTT-TCM formula, it now becomes possible to use the high strength steel experiment data to predict the DWTT energy, and compare the prediction results with tested DWTT energy. Attention should be paid to the constant 'a' in DWTT-TCM, which varies with pipe grade.

Chapter 4

Analysis of Crack Tip Open Angle (CTOA)

4.1 Introduction of CTOA Single-curve Method (CTOA-SCM)

As a result of the parametric study, an interpolation formula for maximum CTOA has been developed for pipeline steels [22], this is given by the general

$$\text{form: } CTOA_{SCM} = C \left(\frac{\sigma_h}{E} \right)^m \left(\frac{\sigma_h}{\sigma_0} \right)^n \left(\frac{D}{t} \right)^q \quad (4.1)$$

m, n and q are dimensionless constants and C is in units of degrees, σ_h : hoop stress in units of MPa, σ_0 : flow stress in units of MPa, D: diameter in units of mm, t: thickness in units of mm.

The author determined in his paper that the following values can be used for methane:

$$C = 106; m = 0.753; n = 0.778; q = 0.65.$$

Therefore the single-curve method for CTOA (CTOA-SCM) is given:

$$CTOA_{SCM} = 106 \cdot \left(\frac{\sigma_h}{E} \right)^{0.753} \left(\frac{\sigma_h}{\sigma_0} \right)^{0.778} \left(\frac{D}{t} \right)^{0.65} \quad (4.2)$$

We checked the validity of the quantities in eqn. (4.2) by fitting the equation to the results of the parametric study typified by those in Table 4-1. The success of the exercise is reflected in Table 4-1 and Figure 4-1.

Table 4-1 data for deriving the constants in eqn. 4.1 ($CTOA_{exp}$, CTOA values from experiment, $CTOA_{calc}$: CTOA calculated from eqn. (4.2))

σ_o (MPa)	σ_h (MPa)	D(mm)	t(mm)	$CTOA_{exp}$	$CTOA_{calc}$, ratio
592	207	762	12.7	3.8	3.654, 0.962
592	207	1067	12.7	3.9	4.547, 1.166
592	207	1067	18.8	3.7	3.526, 0.953
592	207	1422	18.8	3.8	4.246, 1.117
592	310	762	12.7	6.7	6.777, 1.012
592	310	1067	12.7	8.2	8.434, 1.029
592	310	1067	18.8	6.0	6.540, 1.090
592	310	1422	18.8	8.0	7.876, 0.985
592	448	762	12.7	13.0	11.906, 0.916
592	448	1067	12.7	16.8	14.817, 0.882
592	448	1067	18.8	12.5	11.489, 0.919
592	448	1422	18.8	15.5	13.836, 0.893
828	207	762	12.7	3.7	2.813, 0.760
828	207	1067	12.7	3.8	3.500, 0.921
828	207	1067	18.8	3.7	2.714, 0.734
828	207	1422	18.8	3.8	3.268, 0.860
828	310	762	12.7	5.5	5.213, 0.948
828	310	1067	12.7	6.4	6.488, 1.014
828	310	1067	18.8	5.0	5.031, 1.006
828	310	1422	18.8	6.1	6.058, 0.993
828	448	762	12.7	8.5	9.168, 1.079
828	448	1067	12.7	12.1	11.409, 0.943
828	448	1067	18.8	8.2	8.847, 1.079
828	448	1422	18.8	11.5	10.654, 0.926

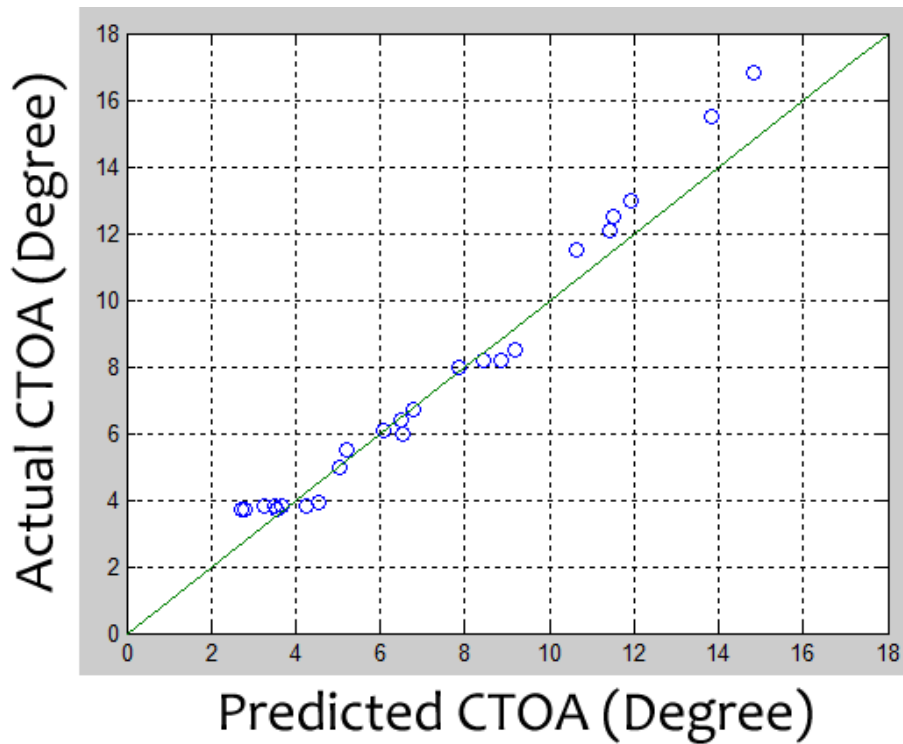


Figure 4-1 Curve fitting of predicted CTOA from eqn.(4.2) and real CTOA value.

4.2 Derivation of Linear relation between CTOA and CVN

Manipulate Eqn. (4.2) to calculate $CTOA_{SCM}$ for the 8 points in our database (section 2.1.1). And compare $CTOA_{SCM}$ to Charpy V-notch energy which is most popular in characterizing the required toughness, the result is shown in Figure 4-2, the corresponding data are listed in Table 4-2.

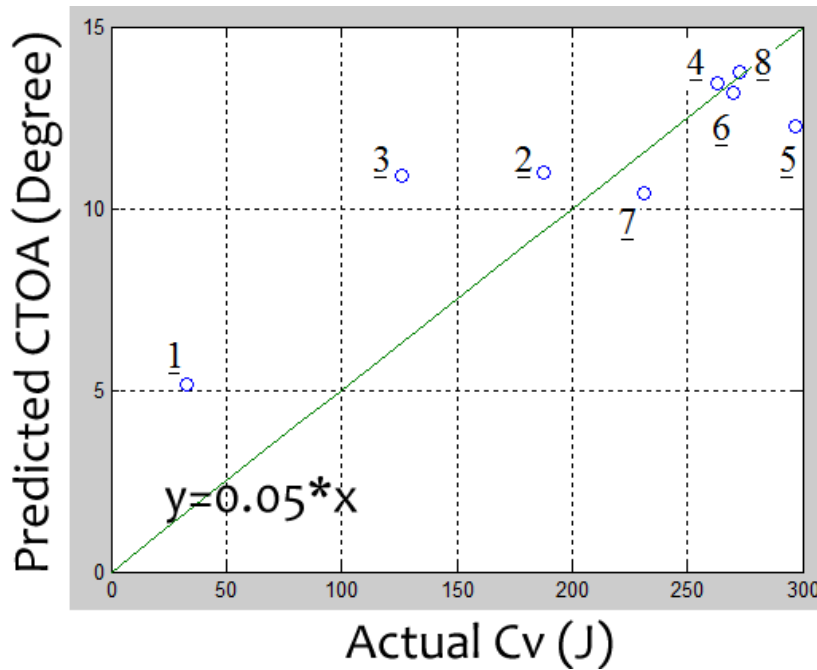


Figure 4-2 The linearity between CTOA-SCM and CVN energy values from experiment.

A linear relation is derived from Figure 4-2:

$$CTOA_{SCM} = 0.05 * C_v \quad (4.3)$$

$CTOA_{SCM}$ in degree and C_v in joule, the linear relation provides a possibility for $CTOA_{max}$ to be used to replace C_v to characterize fracture toughness for line pipes. However, the linearity between CTOA and CVN energy for low grade pipes is poor than the linearity for those high grade pipes.

In the past, CTOA has been manipulated to characterize the fracture toughness for steel pipes, however, since there is no relation between CTOA and CVN energy, the effectiveness for CTOA in charactering fracture toughness as compares to CVN energy cannot be validated. Now the linear relation between CTOA and CVN reveal that CTOA has the same efficiency as CVN energy in characterizing fracture toughness for steel pipes.

The linear eqn. (4.3) shows the similarity between CTOA and CVN energy, however, the difference between this two parameters is, CTOA is more accurate in characterizing high grade pipe toughness but less accurate for low grade case while CVN energy is vice versa.

Table 4-2 Data for deriving the constants in eqn. 4.3. (σ_h : hoop stress, σ_0 : flow stress, D: diameter, t: thickness, $CTOA_{SCM}$: CTOA calculated from eqn. (4.2), C_v : experimental Charpy V-notch energy)

	1	2	3	4	5	6	7	8
$\sigma_0 (MPa)$	482.6	535	541	663	724	750	739	827
$\sigma_h (MPa)$	270.9	386.4	386.4	469.2	517.2	551.5	515.7	595.8
D (mm)	508	1219.2	1219.2	1422.4	914.4	914.4	914.4	914.4
t (mm)	12	18.3	18.3	19.1	16.0	16.0	20.0	16.0
$CTOA_{SCM}$	5.145	10988	10893	13453	12272	13200	10427	13763
$C_v (J)$	325	188	126	263	297	270	252	273

This linear relation between CTOA and CVN is consistent with the simulation result from Ren's report [38], in which the author indicated that a simple linear relation can be deduced to relate CVN energy and steady state CTOA.

Some author concludes that CTOA decreases when crack speed increases [39]-[40], see Figure 4-4. However, after comparing CTOA and crack speed results for the 8 data points we selected, we suggest that this conclusion cannot be applied to our data, see Table 4-3, Figure 4-3.

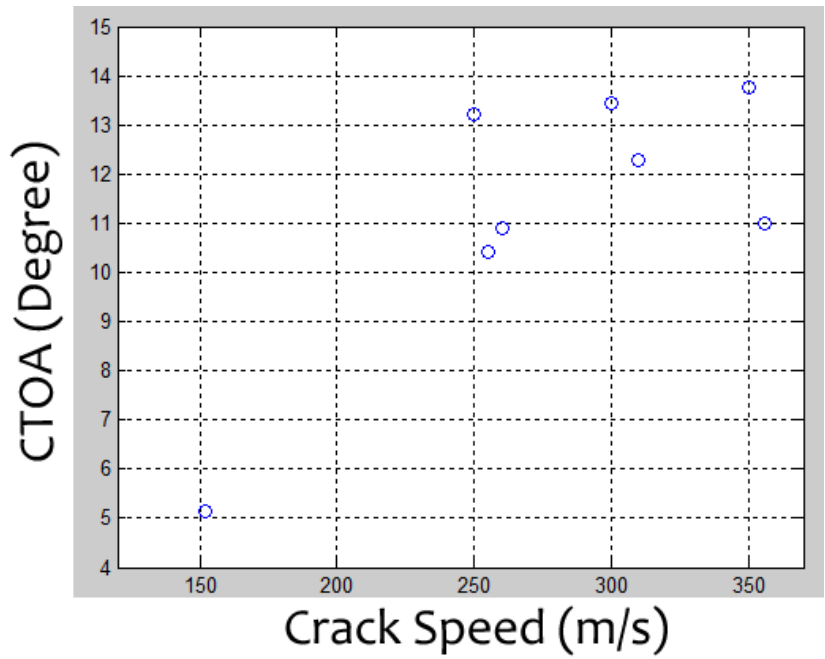


Figure 4-3 The relationship between crack speed and CTOA-SCM.

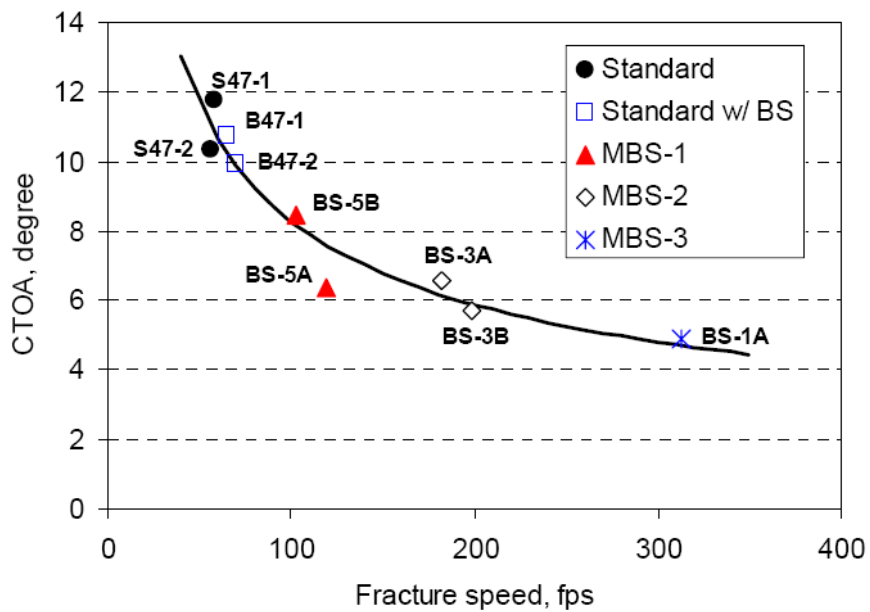


Figure 4-4 The relationship between crack speed and CTOA, from reference

[39].

Table 4-3 comparison between crack speeds and CTOA single-curve method

values. ($CTOA_{SCM}$: CTOA values calculated from eqn. (4.2))

	1	2	3	4	5	6	7	8
Test speed(m/s)	151.8	356	260	300	310	250	255	350
$CTOA_{SCM}$	5.145	10988	10893	13453	12272	13200	10427	13.763

4.3 Derivation of TCM expressed with CTOA (CTOA-TCM)

Similar to DWTT-TCM suggested in section 3.3, we can replace C_v with CTOA to derive a new TCM for CTOA (CTOA-TCM) as follows:

$$\left\{ \begin{array}{l} V_f = 0.617 \times \frac{\sigma_{flow}}{\sqrt{CTOA}} \times \left(\frac{P_d}{P_a} - 1 \right)^{\frac{1}{6}} \\ \frac{P_d}{P_i} = \left[\frac{V_d}{6V_a} + \frac{5}{6} \right]^7 \\ P_a = \frac{4}{3.33\pi} \cdot \frac{t}{D} \cdot \sigma_{flow} \cdot \cos^{-1} \exp \left(\frac{-375 \cdot \pi E \cdot CTOA}{24\sqrt{Dt} / 2 \cdot \sigma_{flow}^2} \right) \end{array} \right. \quad (4.4)$$

By manipulating Eqn. (4.4), we can use the crack speed to calculate CTOA, or input CTOA values to get the crack speed.

The accuracy of this formula is as same as the classical TCM characterized with Charpy energy, therefore worse than that of the CTOA-SCM:

$$CTOA_{SCM} = 106 \cdot \left(\frac{\sigma_h}{E} \right)^{0.753} \left(\frac{\sigma_h}{\sigma_0} \right)^{0.778} \left(\frac{D}{t} \right)^{0.65} \quad (4.2)$$

However, the use of CTOA to characterize fracture toughness for steel pipes is not completely accepted by all researchers, because the definition of CTOA in experiments is not clear up until now. Since we know that crack tip angle is not always symmetric, when it becomes dissymmetric, the exact angle of CTOA is still under debate.

4.4 Comparison between CTOA-SCM, Battelle-TCM, LS-TCM, Maxey-SCM and Vogt-SCM:

Combine the linear relation between CTOA and CVN energy we derived in previous section (eqn.(4.3)) with the CTOA-SCM (eqn.(4.2)), we can get a new Charpy V-notch energy formula, to convert the CTOA values in degree to CVN energy values in Joule:

$$C_{v-CTOA} = 2120 \cdot \left(\frac{\sigma_h}{E}\right)^{0.753} \left(\frac{\sigma_h}{\sigma_0}\right)^{0.778} \left(\frac{D}{t}\right)^{0.65} \quad (4.5)$$

The purpose for deriving Eqn. (4.5) is to compare CTOA values directly with CVN values calculated by theoretical methods, because we have CTOA values in “Joule” now, see Table 4-4 and Figure 4-5.

Table 4-4 Comparison of the fracture toughness calculated from different formulas ($CTOA_{SCM}$: CTOA calculated from eqn. (4.2), C_{v-CTOA} : fracture toughness calculated from eqn. 4.5)

	1	2	3	4	5	6	7	8
--	---	---	---	---	---	---	---	---

Test toughness(J)	32.5	188	126	263	297	270	252	273
$CTOA_{SCM}$	5.145	10988	10893	13453	12272	13200	10427	13763
C_{v-CTOA} (J)	102.9	219.8	217.86	269.1	245.4	264.0	200.5	275.3
Battelle-TCM tough(J)	31.8	99.2	99.9	163.4	169.6	146.5	126.2	163.3
Maxey-SCM toughness(J)	37.9	118.8	118.8	187.0	185.0	210.3	198.1	245.4
Vogt-SCM toughness(J)	36.4	132.0	132.0	221.7	224.3	260.5	247.4	311.8
LS-TCM toughness (J)	31.7	146.1	110.7	249.9	226.6	230.0	267.3	283.3

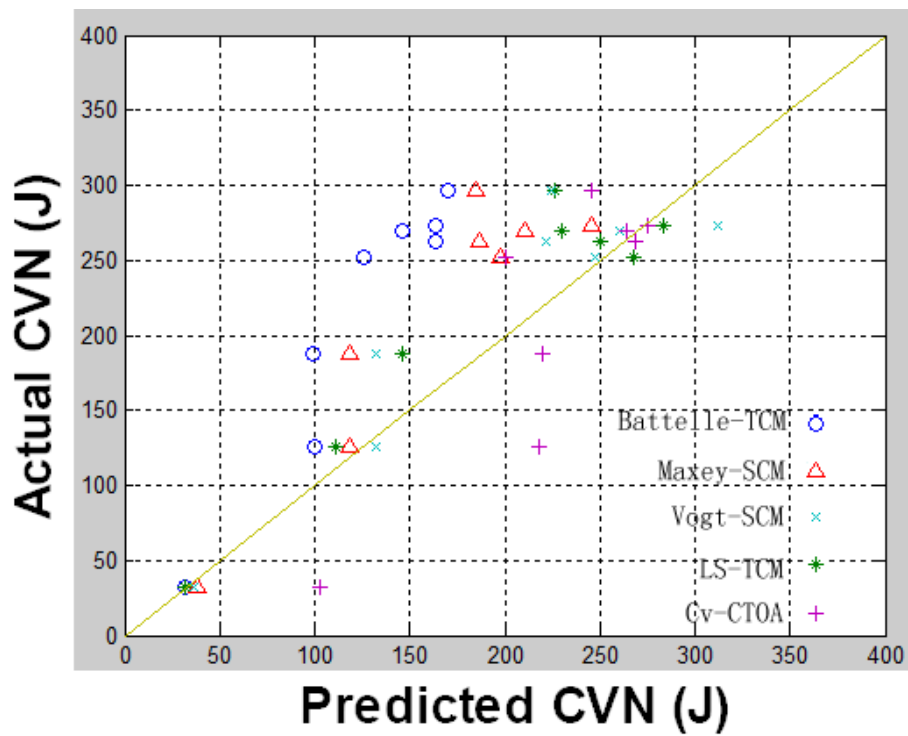


Figure 4-5 Comparison of fracture toughness calculated from different formulas.

By comparing the fracture toughness characterized by Charpy energy calculated from different formulas, see Table 4-4 and Figure 4-5, we find that C_{v-CTOA} is better than Battelle-TCM and Maxey-SCM in predicting high grade toughness, even better than the toughness predicted by Vogt-SCM and

LS-TCM. The reason why C_{v-CTOA} is more accurate than single-curve methods may be due to the fact that C_{v-CTOA} manipulates 4 parameters while single-curve methods only use 3 parameters.

Furthermore, due to the simplicity of CTOA values to be observed in high speed crack propagation experiments, C_{v-CTOA} may be used for predicting fracture toughness in high crack speed cases.

However, the limitation for C_{v-CTOA} is, it is not accurate for predicting low grade pipe toughness, therefore, CTOA cannot be used for fracture toughness characterization for low grade pipes. Low grade pipe toughness values can only be characterized by CVN energy and DWTT energy.

CTOA value, together with CVN energy and DWTT energy, are all potential candidates to characterize high strength steel pipe toughness. Furthermore, the fracture toughness characterized by CTOA-SCM is comparable to that from LS-TCM and Vogt-SCM, as is shown in this section.

4.5 Remarks

In section 4.1, the validity of CTOA-SCM is discussed based on available CTOA data.

In section 4.2, a linear relationship is obtained between CTOA and CVN energy from known low and high grade pipe data, which provides the possibility for CTOA to be used as a comparable parameter with CVN and DWTT energy, to characterize the fracture toughness. The linear relation

between CTOA and CVN reveal that CTOA has the same accuracy as CVN energy in characterizing fracture toughness for steel pipes. This linear relationship is validated by a simulation result about CTOA and CVN energy from reference paper [39].

In section 4.3, a new TCM is derived based on the linear relation between CTOA and CVN, so as to be called the CTOA-TCM. We can use the crack speed to calculate CTOA, or put CTOA value forward to get the crack speed.

In section 4.4, it is shown that the CTOA-SCM is comparable to LS-TCM and Vogt-SCM in characterizing the fracture toughness according to currently available high grade pipe data. CTOA value, together with CVN energy and DWTT energy, are all potential candidates to characterize high strength line pipe toughness. However, CTOA values are not accurate when used to predict fracture toughness values for low grade pipes.

Chapter 5

Summary and Future Work

5.1 Summary of the thesis

Four new methods, LS-TCM, DWTT-SCM, DWTT-TCM and CTOA-TCM are proposed and compared with known high grade pipe data; two existed methods, Vogt-SCM and CTOA-SCM are introduced and validated, in order to facilitate the characterization and calculation of high grade pipe fracture toughness. All these methods together lead to a systematical characterization and calculation methodology for high grade pipe fracture toughness based on three variables, CVN, DWTT and CTOA.

The importance of Charpy V-notch energy is enhanced in this thesis. The concept of “limit (crack) speed” is introduced, and a new limit speed-based two-curve method (LS-TCM) is proposed to compensate the non-conservative weakness of the original Battelle TCM in characterizing the CVN energy for high grade pipes, LS-TCM gives accurate predictions of CVN energy as compared to available high/low grade pipe test results. Vogt-SCM is chosen instead of original Maxey-TCM, because it is a better single-curve method in characterizing CVN energy according to current high grade pipe data. Linear relationships between DWTT-CVN and CTOA-CVN are proposed, which facilitate the conversion and comparison of the other two fracture toughness parameters, DWTT energy and CTOA with CVN energy, to further enhance the importance of CVN energy as the basic variable in characterizing fracture toughness of line pipes.

The single-curve method and two-curve method for DWTT energy,

DWTT-SCM and DWTT-TCM are proposed. A linear relationship is found between the DWTT energy calculated using DWTT-SCM and the CVN energy calculated using Vogt-SCM, which makes it easy to convert between DWTT and CVN energy for both low and high grade pipes, thus facilitate the DWTT energy to be used in future fracture toughness calculation. A comparison between linear and non-linear formulas for DWTT-CVN relation is done, which shows that linear formula better characterize the relation between DWTT energy and CVN, however the constant in the linear DWTT-CVN formula decreases when pipe grade increases.

The single curve method for CTOA (CTOA-SCM), which is derived before for characterizing low grade pipe toughness, is shown to be applicable for characterizing fracture toughness for known high grade pipe data, while a new CTOA two-curve method (CTOA-TCM) is derived between CTOA and CVN. A linear relationship is obtained between CTOA and CVN energy, which shows that CTOA has the same accuracy as CVN energy in characterizing fracture toughness for steel pipes. It is also showed that CTOA is accurate in predicting fracture toughness for high grade pipes but not for low grade pipes.

5.2 Future work

In the future, attention could be paid to a series of questions:

1. Our derivation of LS-TCM is based on the new fracture propagation experiments, further experiments about high grade pipes, especially of grade X100 or higher will provide more high grade pipe toughness data, which help us to improve the LS-TCM and our calculation methodology of high grade pipes.

2. In LS-TCM, we only modify the crack speed equation compares to Battelle-TCM. The modifications of the other two equations are also possible. For the arrest pressure equation, there was a simple assumption of uniform yield stress at the crack tip, if we change it to any non-uniform distribution, then the situation at crack tip become more realistic. For the gas equation, constants can be changed because the composition and density of new nature gas transmitted by line pipes is different from that of the past.

3. We introduced a DWTT-TCM, however, this method is based on the linear relation between DWTT and CVN energy, we also notice that the constant in the DWTT-CVN linear equation changes with pipe grade. Therefore it is possible to introduce a new DWTT-TCM, which is not based on CVN, to improve the calculation of DWTT energy.

4. Further high grade pipe data are needed to improve the CTOA-SCM, we tried to modify the CTOA-SCM but failed, because we can only find 3-4 CTOA data for high grade pipes, when we put the 3-4 data together, we find that the scattering is too large to derive a real equation. If further high grade pipe CTOA data are provided, we can change this CTOA-SCM to better represent fracture toughness for both low and high grade line pipes.

Bibliography

- [1] R. Andrews, A. Batte, Developments in fracture control technology for gas pipelines utilising high strength steels.
- [2] K. Corbett, R. Bowen, C. Petersen, High Strength Steel Pipeline Economics, International Journal of Offshore and Polar Engineering, 14(2004), p.105-112.
- [3] H. Hillenbrand, A. Liessem, C. Kalwa, M. Erdelen-Pepler, C. Stallybrass, Technological solutions for high strength gas pipelines.
- [4] H. Hillenbrand, M. Graf, C. Kalwa, Development and production of high strength pipeline steels, Niobium 2001, Orlando, USA.
- [5] H. Hillenbrand, C. Heckmann, K. Niederhoff, X80 line pipe for large-diameter high strength pipelines, APIA 2002 Annual Conference, (2002).
- [6] I. Takeuchi, H. Makino, S. Okaguchi, N. Takahashi, A. Yamamoto, Crack arrestability of high-pressure gas pipelines by X100 or X120, 23rd World Gas Conference, Amsterdam, (2006).
- [7] R. Eiber, T. Bubenik, W. Maxey, Fracture control technology for natural gas pipelines, To Line Pipe Research Supervisory Committee of the Pipeline Research Committee of the American Gas Association, (1993).
- [8] W. Maxey, Fracture initiation, propagation and arrest, Applied Mechanics of Materials Section Battelle's Columbus Laboratories.
- [9] T. Goodier, F. Field, Fracture of Solids, Interscience Publishers, Inc., New York(1963), p.103.
- [10] H. Liepmann, A. Roshko, Elements of gasdynamics, John Wiley & Sons Inc., (1957).
- [11] C. Shen, Fracture Mechanics, Tongji University Press, (1996).
- [12] J. Wolodko, M. Stephens, Applicability of Existing Models for Predicting Ductile Fracture Arrest in High Pressure Pipelines, International Pipeline Conference, (2006), Calgary, Alberta, Canada .

- [13] G. Wilkowski, D. Rudland, H. Xu, N. Sanderson, Effect of Grade on Ductile Fracture Arrest Criteria for Gas Pipelines, Proceedings of International Pipeline Conference, (2006).
- [14] G. Mannucci, G. Demofonti, D. Harris, L. Barsanti, H.G. Hillenbrand, Fracture Properties of API X100 Gas Pipeline Steels. Proceedings from 13th Biennial Joint Technical Meeting, (2001).
- [15] B. Leis, R. J. Eiber, L. Carlson, A. Gilroy-Scott, Relationship Between Apparent (Total) Charpy ee-Notch Toughness and the Corresponding Dynamic Crack-Propagation Resistance. International Pipeline Conference - Volume II, ASME, (1998).
- [16] S. Papka, J. Stevens, M. Macia, D. Fairchild, C. Petersen, Full-Size Testing and Analysis of X120 Line pipe. Proceedings of 13th International Offshore and Polar Engineering Conference, (2003).
- [17] G. Wilkowski, W. Maxey, R. Eiber, A.G.A./API Drop Weight Tear Test Round Robin Testing Program, PRCI Catalogue No. L51471, (1985).
- [18] Ryota Higuchi, Hiroyuki Makino, New Concept and Test Method on Running Ductile Fracture Arrest for High Pressure Gas Pipeline, (2005).
- [19] G. Wilkowski, W. Maxey, R. Eiber, Use of a Brittle Notch DWTT Specimen to Predict Fracture Characteristics of Line Pipe Steels. Proceedings of the Energy Technology Conference, 19(1980), p.59-77.
- [20] T. Ishihara, J. Kondo, T. Kikada, T. Akiyama, Drop Weight Tear Test of Linepipe Materials By Using Laterally Compressed Specimen, Presented to the 110th ISIJ Meeting, October 1985, 51379, at Niigata University in Niigata.
- [21] D. Shim, G. Wilkowski, D. Duan, J. Zhou, Effect of Fracture Speed on Ductile Fracture Resistance: Part 1—Experimental, 8th International Pipeline Conference, (2010), p.539-545.
- [22] L. Pussegoda, S. Verbit, A. Dinovitzer, W. Tyson, A. Glover, L. Collins, L. Carlson, J. Beattie, Review of CTOA as a measure of ductile fracture toughness, Proceedings of International Pipeline Conference, (2000).
- [23] P. O'Donoghue, M. Kanninen, C. Leung, G. Demofonti, S. Venzi, The

development and validation of a dynamic fracture propagation model for gas transmission pipelines, *International Journal of Pressure Vessels and Piping*, 70(1997), p.11–25.

[24] Z. Li, C. Turner, Crack-Opening Angle and Dissipation-Rate Analysis of R-Curves for Side Grooved Pieces of HY 130 Steel in Bending, *Jour. Material Science*, 28(1993), p.5922-5930.

[25] McCoy, N. James, C. Echometer, Acoustic Velocities for Natural Gas, *Society of Petroleum Engineers*, (1974).

[26] E. Sugie, M. Matsuoka, T. Akiyama, K. Tanaka, Y. Kawaguchi, Notch Ductility Requirements of Line Pipes for Arresting Propagation Shear Fracture, *Journal of Pressure Vessel Technology*, ASME, 109(1987), p.424-434.

[27] G. Demofonti, G. Mannucci, C.M. Spinelli, L. Barsanti, H.G. Hillenbrand, Large Diameter X100 Gas Linepipes : Fracture Propagation Evaluation by Full-Scale Burst Test, 3rd International Pipeline Technology Conference, Belgium, I(2000), p.509-520.

[28] L. Barsanti, G. Mannucci, H.G. Hillenbrand, G. Demofonti, D. Harris, Possible Use of New Materials for High Pressure Linepipe Construction: An Opening on X100 Grade Steel, 4th International Pipeline Conference, Calgary, (2002), p.287-298.

[29] G. Demofonti, G. Mannucci, H.G. Hillenbrand, D. Harris, Evaluation of the suitability of Evaluation of X100 steel pipes for high pressure gas transportation pipelines by full scale tests, International Pipeline Conference, Calgary, Canada, (2004).

[30] S. Papka, J. Stevens, M. Macia, D. Fairchild, C. Petersen, Full-Size Testing and Analysis of X120 Linepipe, Symposium on High Performance Materials in Offshore Industry, ISOPE, Honolulu, (2003), p.50-59.

[31] M. Lu, Y. Mai, On fast fracture in an elastic-(plastic)-viscoplastic solid Part II – The motion of crack, *International Journal of Fracture* 129(2004), p.177–195.

[32] Ryota Higuchi, Hiroyuki Makino, New Concept and Test Method on

- Running Ductile Fracture Arrest for High Pressure Gas Pipeline, (2005).
- [33] W. Maxey, J. Kiefner, R. Eiber, Ductile Fracture Arrest in Gas Pipelines, American Gas Association, Catalog No. L32176, (1975).
- [34] AISI Technical Report, Running Shear Fractures in Line Pipe, Subcommittee of Large Diameter Line Pipe Producers, (1974).
- [35] G. Feanehough, D. Jones, Toughness Specification for Shear Fracture Arrest in Pipelines, International Conference on Analytical and Experimental Fracture Mechanics, (1980), p.23-27.
- [36] G. Vogt, et al, EPRG Report on Toughness for Crack Arrest in Gas Pipelines, 3R International, 22(1983), p.98-105.
- [37] G. Wilkowski, W. Maxey, R. Eiber, Use of the DWTT Energy for Predicting Ductile Fracture Behavior in Controlled-Rolled Steel Line Pipes, Canadian Metallurgical Quarterly, 19(1980), p.59-77.
- [38] Z. Ren, C. Ru, Second Year' s Report : Finite Element Analysis of Speed - Dependent Ductile Fracture Toughness in DWTT, University of Alberta, (2012) 16 pages.
- [39] D. Shim, G. Wilkowski, D. Duan, J. Zhou, Effect of Fracture Speed on Ductile Fracture Resistance: Part 1—Experimental, 8th International Pipeline Conference, 2(2010), p. 539-5
- [40] D. Rudland, G. Wilkowski, Z. Feng, Y. Wang, D. Horsley, A. Glover, Experimental investigation of CTOA in line pipe steels, Engineering Fracture Mechanics, 70(2003), P. 567–577.